QUALITY ASSURANCE OF CONCRETE USING ELECTRICAL RESISTIVITY MEASUREMENTS

by

Matthew C. MacArthur

BScE, University of New Brunswick, 2010

A Report Submitted in Partial Fullfillment
of the Requirements for the Degree of

Master of Engineering

In the Graduate Academic Unit of Civil Engineering

Supervisor: Michael D.A. Thomas, PhD, P.Eng., Department of Civil Engineering

Readers: Peter H. Bischoff, PhD, P.Eng., Department of Civil Engineering
Xiomara Sanchez, PhD, P.Eng., Department of Civil Engineering

This report is accepted by the Dean of Graduate Studies

THE UNIVERSITY OF NEW BRUNSWICK

February, 2019

ABSTRACT

This study was focused on evaluating the use of electrical test methods to evaluate the permeability of concrete in New Brunswick Department of Transportation and Infrastructure (NBDTI) structures and various laboratory-produced samples. Many transportation departments currently use the Rapid Chloride Ion Penetrability (RCP) test (ASTM C1202) to evaluate concrete placed in highway structures as a means of quality assurance. In this study, concrete samples were taken from thirteen (13) separate NBDTI bridge projects and six (6) laboratory (lab) mixes. All samples were cast on-site or in the lab, cured in similar conditions and tested for surface resistivity (SR), bulk resistivity (BR), bulk conductivity (BC) (ASTM C1760) and RCP at an age of 56 days. In-situ SR testing was also performed on three separate structures and compared to values obtained on samples cured in lab conditions.

This study concludes that a good correlation exists between results obtained by SR, BR, BC and RCP testing. These test results indicate that electrical resistivity testing (SR, BR or BC) could be adopted as a substitution for the RCP (ASTM C1202) test for quality assurance testing using lab-cured cylinders.

The small sample set of in-situ SR test results proved too variable to determine the viability of consistent quality assurance specifications without further testing and development of concise correction factors.

DEDICATION

I would like to dedicate this report to my wife, Sarah. I could not have done this without your continuous support and encouragement. You have listened to more discussions regarding concrete than anyone outside of the field of civil engineering should ever have to endure and deserve an honorary degree for doing so. I would also like to dedicate this report to my newborn son, Ben. Planning for your birth gave me the focus to finally complete the final stages of this research so that I can dedicate my focus solely to be the best father to you that I can.

ACKNOWLEDGEMENTS

I would like to acknowledge and thank all of those who have helped and provided their guidance throughout the duration of this project. First and foremost, I would like to thank Dr. Michael Thomas for giving me the opportunity to perform this research under his world class guidance and expertise. I would also like to thank my employer, the New Brunswick Department of Transportation and Infrastructure, and more specifically, my immediate supervisor, Bruce Connolly, for supporting me throughout this journey and providing the necessary tools and research materials to complete this project. Finally, I would like to thank my former colleague, Fred Strang, who encouraged me to further my education in the field of concrete materials.

TABLE OF CONTENTS

LIST OF TABLES

LIST OF FIGURES

LIST OF SYMBOLS, NOMENCLATURE OR ABBREVIATIONS

A	Cross-sectional area (m^2, cm^2 or mm^2)
AC	Alternating Current
AAR	Alkali Aggregate Reactivity
AASHTO	American Association of State Highway Transportation Officials
ASTM	American Society for Testing and Materials
BC	Bulk Conductivity
BR	Bulk Resistivity
C_o	Surface chloride concentration
C_t	Threshold chloride concentration
CCIL	Canadian Council of Independent Laboratories
CNI	Calcium Nitrite – Corrosion Inhibiting Concrete Admixture
CSA	Canadian Standards Association
C-XL	Exposure class for structurally reinforced concrete exposed to chlorides and other severe environments with higher durability expectations (CSA A23.1, 2014)
d	Diameter (m, cm or mm)
D_a	Apparent Diffusion Coefficient (m^2/s)
DC	Direct Current
$E_{\alpha,\rho}$	Activation energy (J/mol)
FA	Fly Ash
Fe	Iron
$Fe(OH)_2$	Rust
FDOT	Florida Department of Transportation
FHWA	Federal Highway Administration
GU	General Use Portland Cement
H_2	Dihydrogen
H_2O	Water
HPC	High Performance Concrete
I	Electric current (mA)
I_o	Electrical current at time = 0 (mA)
I_1	Electrical current measured at 1 minute (mA)
K	Cell constant correction factor for SR (1.95)
L	Length (m, cm or mm)
LADOTD	Louisiana Department of Transportation and Development
N	mols
NaCl	Sodium Chloride
NaOH	Sodium Hydroxide
NBDTI	New Brunswick Department of Transportation & Infrastructure
NJDOT	New Jersey Department of Transportation
OH^-	Hydroxyl Ions

PC	Portland Cement
pH	Logarithmic scale used to specify acidity (0 to 14)
Q	Total charge (coulombs)
Q_s	Equivalent charge passed through a 3.75-inch diameter specimen (coulombs)
Q_x	Charge passed through x diameter specimen in inches (coulombs)
R	Resistance (Ohms or Ω)
R	Gas Constant (8.314 J/mol K)
R^2	Statistical coefficient of determination
RCON™	Proprietary device developed by Giatec Scientific to measure Bulk Resistivity – Trade Mark Name
RCP	Rapid Chloride Ion Penetrability Test (ASTM C1202)
RIME	Rutgers Infrastructure Monitoring and Evaluation Group
SCM	Supplementary Cementitious Material
SF	Silica Fume
SR	Surface Resistivity
t_i	Time to corrosion initiation according to Fick's 2nd law
T	Temperature (Kelvin)
T_o	Reference temperature (Kelvin)
UNB	University of New Brunswick
V	Electrical potential (volts)
V_{50mm}	Volume of a 50mm length, 100mm diameter concrete cylinder
V_{200mm}	Volume of a 200mm length, 100mm diameter concrete cylinder
W/CM	Water-to-cementitious materials ratio
X_d	Depth of reinforcing steel embedment (m)
Ω	Ohms
σ	Electrical conductivity (mS/m)
ρ	Electrical resistivity (kΩ-cm or Ω-m)
ρ_o	Electrical resistivity at the reference temperature (kΩ-cm or Ω-m)
ρ_t	Electrical resistivity at the measured temperature (kΩ-cm or Ω-m)
ρ_{23}	Electrical resistivity at a baseline temperature of 23°C (kΩ-cm or Ω-m)

1 INTRODUCTION

1.1 Background Information

Modern bridge structures in the world are frequently constructed entirely, or at least by portion of, reinforced concrete. Concrete is inherently great in compression, however its resistance to tensile forces is considerably less than that of structural steel. Steel is therefore embedded into concrete to enable it to resist tension to solve this problem; however, doing this creates another problem. Carbon steel, which comprises most of all the reinforcing steel used in concrete, can be very susceptible to corrosion due to chloride ingress from sources such as de-icing salts that can permeate through concrete over time.

In areas of the world such as Canada, where the cold weather and snow during the winter months demand the use of de-icing salts to provide safe travel for vehicles, the protection of the reinforcing steel is of great concern. The portion of concrete that separates the outer most reinforcing steel from the external environment is referred to as concrete cover, and usually accounts for anywhere from 50-mm to 75-mm of concrete in transportation structures. The rate at which chlorides from de-icing salts transport through the concrete cover and initiate corrosion of the reinforcing steel is largely dependent on the degree of permeability, and therefore the quality of the concrete itself. The permeability of the concrete material, or the rate at which chlorides can diffuse through the concrete material, is dependent on many basic concrete fundamentals such as the water to cementitious materials ratio (w/cm) and the use of supplementary cementing materials such as fly ash, slag and silica fume. Other factors, such as the

exposure environment, finishing, workmanship, curing, age and various types of cracking also play an important role (ASTM C1556, 2016).

The majority of the concrete mixes that are used for bridge structures constructed by the New Brunswick Department of Transportation and Infrastructure (NBDTI) are designed to meet the requirements of CSA A23.1-14 exposure class C-XL (concrete exposed to chlorides in an extreme environment). The specification as of the 2014 edition of CSA A23.1 for C-XL exposure class concrete is briefly summarized in Table 1.1.

Table 1.1: Summary of C-XL Specification in CSA A23.1-14

CSA A23.1-14 Exposure Class C-XL Concrete	
w/cm	<0.40
Compressive Strength	50 MPa within 56 Days
RCP (ASTM C1202)	<1000 C @ 91 Days

The Rapid Chloride Ion Penetrability (RCP) Test (ASTM C1202, 2018), is a test method that is currently in use by many transportation agencies, including NBDTI, to indicate the chloride resistance of a concrete sample by electrical response (Ghosh and Tran, 2015). During the test, an electric potential of 60 volts is applied across a 50-mm slice sawn from a 100-mm diameter concrete cylinder over a period of six hours, and its electrical charge (in coulombs) that passes through the specimen is determined. To briefly summarize, the larger the amount of charge passed through the concrete specimen over the six-hour period is indicative of concrete with increased permeability

and therefore a material more susceptible to chloride ingress. Table 1.2 depicts the typical ranges of charge passed through a sample and its corresponding degree of chloride ion penetrability.

Table 1.2: Chloride Ion Penetrability Based on Charge Passed (ASTM C1202, 2018)

Charge Passed (coulombs)	Chloride Ion Penetrability
>4000	High
2000-4000	Moderate
1000-2000	Low
100-1000	Very Low
<100	Negligible

In recent years, other non-destructive electrical techniques to provide an indication of a concretes resistance to chloride ingress are beginning to emerge and gain acceptance in the industry. Such methods are Surface Resistivity (SR) testing and Bulk Resistivity (BR) testing. These developing test methods have shown time and cost savings due to shorter testing times as well as increased accuracy (Nassif et al., 2015; Icenogle and Rupnow, 2011).

The ability to measure the permeability of concrete in-situ, rather than from a lab-cured sample also provides many advantages to specifiers and owners. Samples have traditionally been taken during the placement of concrete in a structure, cured on site in a temperature-controlled curing box at 15 to 25 degrees Celsius for 20 to 36 hours, and

then moved to a temperature-controlled lab-curing environment of 21 to 25 degrees Celsius until the time of testing as per CSA A23.2-3C. An age of 56 days for testing is specified by NBDTI for RCP testing. The controlled laboratory curing environment is often quite different than the curing environment of the job site in terms of temperature and moisture treatment. This job-site variation often has little effect on the portions of concrete beneath the surface, or concrete cover (ACI 308R-16, 2016). However, the curing affected zone within 50-mm to 75-mm of concrete that protects the reinforcing steel from chloride ingress and ultimately corrosion, cracking, spalling and rehabilitation or replacement is dependent on the curing treatment at an early age. This outer portion of concrete is critical to the service life of a structure. A measure of this concrete in-situ, rather than from an optimally lab cured cylinder, has the potential to measure actual construction performance, rather than the potential of a concrete mix design based on lab cured results.

1.2 Project Scope

In this study, the RCP test (ASTM C1202) will be used as a benchmark to evaluate the potential use of surface resistivity (SR), bulk resistivity (BR) and bulk conductivity (BC) as alternative test methods to accurately indicate the permeability of concrete as a quality assurance measure. Concrete samples were produced in the field from various NBDTI bridge projects, as well as from concrete samples of various mix designs produced in the UNB laboratory. A total of 92 samples were tested by the following test methods:

- Rapid Chloride Ion Penetration Test (ASTM C1202, 2018)
- Surface Resistivity Test (AASHTO TP95-14, 2014)

- Bulk Resistivity Test (ASTM Draft 7, Dated June 12, 2015)
- Bulk Conductivity (ASTM C1760, 2012)

The above testing methods were evaluated against each other to determine cost effective and accurate test methods to supplement or replace the use of RCP Testing.

In addition to lab testing, SR measurements were taken from a small sample set of newly constructed bridge structures using a Wenner type 4-point probe to measure surface resistivity of concrete in-situ. An evaluation as to whether surface resistivity testing can be used as an accurate tool for quality assurance (QA) testing on concrete placed and cured in an actual structure, as opposed to lab cured cylinders, will be based on these test results and a review of the literature.

2 LITERATURE REVIEW

2.1 Chloride Induced Corrosion

Reinforcing steel embedded in concrete benefits from a passivation layer on its surface that is establishes itself soon after cement hydration begins. This passivation layer is established due to the high alkalinity of concrete, which has a pH of approximately 13. However, chloride ions permeating into the concrete in the presence of oxygen and water can destroy the passivation layer, thus initiating corrosion (Thomas, CE 6563 Course Notes, 2014; Neville, 2011).

For corrosion of the reinforcing steel to occur, there must be 1) an anodic site on the reinforcing steel to release electrons 2) a cathodic site to consume the electrons released by the anodic site, 3) an electrolyte, which is provided by the concrete pore solution, to conduct the ionic current flow between the anodic and cathodic sites, and 4) an electric circuit to complete the flow of electrons, which is provided by the reinforcing steel. Equation 2.1 describes the reaction at the anodic site, releasing electrons. Equation 2.2 describes the reaction at the cathodic site, consuming the electrons released by the anodic site and combining with water and oxygen to form hydroxyl ions $(OH)^-$ (Thomas, CE 6563 Course Notes, 2014; Neville, 2011).

$$Fe \rightarrow Fe^{2+} + 2e^- \qquad \textbf{Eq. 2.1}$$

$$H_2O + {}^1\!/_2\, O_2 + 2e^- \rightarrow 2(OH)^- \qquad \textbf{Eq. 2.2}$$

The iron ($\boldsymbol{Fe^{2+}}$) and hydroxyl ions $(\boldsymbol{OH})^-$ produced by Equations 2.1 and 2.2 cause a further reaction described in Equation 2.3, resulting in the formation of rust ($\boldsymbol{Fe(OH)_2}$) on the reinforcing steel. This corrosion and rust formation occupies a volume much larger than the original reinforcing steel. When the pressure resulting from this increase in volume exceeds the tensile strength of the concrete, cracking is initiated which can further result in delamination and spalling of the concrete (Thomas, CE 6569 Course Notes, 2014; Neville, 2011).

$$\boldsymbol{Fe^{2+} + 2OH^- \rightarrow Fe(OH)_2} \qquad \textbf{Eq. 2.3}$$

2.2 Predicting the Time to Corrosion Initiation

The service life of a steel reinforced concrete transportation structure is the period of time in which a structure performs its intended design function without unforeseen maintenance and repair (CAN/CSA S6, 2006). The service life is strongly dependent on the ability of the structure to resist deterioration from various forms of mechanisms such as alkali aggregate reaction (AAR), carbonation, and corrosion to name a few. In marine environments, or in geographical locations where the use of deicing salts is necessary, corrosion of the reinforcing steel is often a primary mechanism of structure deterioration.

Extending the time elapsed from the time of construction until corrosion of the reinforcing steel is initiated, also referred to as the time to corrosion, is critical for a reinforced concrete structure to fulfill its intended service life. The longer this period from the time of construction until corrosion of the reinforcing steel is initiated, the

longer the service life of the structure itself which will ultimately result in reduced maintenance and repair costs.

The time to corrosion initiation of the reinforcing steel is dependent on the quality and thickness of the concrete cover protecting the reinforcing steel as well as the environment in which the structure is located. Concrete quality can be directly related to its ability to resist the transmission of aggressive ions through its pore structure, often referred to as its degree of permeability or chloride resistance. The chloride resistance of a saturated concrete refers to its ability to protect reinforcing steel from corrosion, and is dependent upon its pore structure and the composition of the cement hydrates. The volume and size of the pores, as well as the degree of tortuosity of the pore structure play an important role in resisting the transmission of chlorides through a concrete material. The composition of the cement hydrates play an important role in their ability to bind chlorides (Thomas, CE 6503 Course Notes, 2014).

The time at which corrosion of the reinforcing steel is initiated can be modeled using Fick's second law of diffusion, a mathematical solution which is presented as Equation 2.4. The time to corrosion initiation, $\boldsymbol{t_i}$, is a function of the chloride content at the surface, $\boldsymbol{C_0}$, the threshold chloride content required to initiate corrosion, $\boldsymbol{C_t}$, the apparent diffusion coefficient of the concrete, $\boldsymbol{D_a}$, and the depth of cover to the reinforcing steel, $\boldsymbol{x_d}$ (Thomas, CE 6503 Course Notes, 2014). The error function, within Fick's second law equation, $\boldsymbol{erf(z)}$, is defined in Equation 2.5 (ASTM C1556-11a, 2016).

$$C_t = C_0 \left[1 - erf\left(\frac{x_d}{2\sqrt{D_a t_i}}\right)\right] \quad \textbf{Eq. 2.4}$$

$$erf(z) = \frac{2}{\sqrt{\pi}} \int_0^z exp(-u^2) du \quad \textbf{Eq. 2.5}$$

2.3 Test Methods to Directly Measure Concrete Permeability

Test methods such as the Penetration of Chloride Ion into Concrete by Ponding (ASTM C1543-10a, 2010) and the method of determining the Apparent Chloride Diffusion Coefficient by Bulk Diffusion (ASTM C1556-11a, 2016) are standardized test methods that are direct measures of concrete permeability.

ASTM C1556 determines the apparent chloride diffusion coefficient, D_a (m^2/s), of a concrete sample by immersing it in sodium chloride solution for a period of at least 35 days after initial curing. Longer immersion times are required for concretes of higher quality, such as high-performance concrete (HPC). The sample is then ground at prescribed depth intervals to determine the acid-soluble chloride contents at increasing depth. Once the chloride concentrations at both the surface and various depths are determined, they are plotted against the depth from the surface. Fick's second law of diffusion is then used to curve fit to the measured chloride contents by means of non-linear regression analysis using the method of least squares, determining the apparent chloride diffusion coefficient, D_a, that best fits the equation (ASTM C1556-11a, 2016). CSA A23.2-14, Annex J, states that this test method takes a minimum of 75 days to complete, considering curing of the sample, immersion time and completion of the test.

Longer times are required if curing is to extend beyond 28 days and if there is a need to extend the immersion time beyond 35 days for HPC mixes.

ASTM C1543 determines the penetration of chloride ions into concrete by ponding. Slabs of at least 0.03m^2 in area and a thickness of 75-mm to 105-mm are cast, cured for a time period of 14 days unless otherwise specified, then allowed to dry at 50% relative humidity for another 14 days. Once the drying period is complete, the slabs are ponded with sodium chloride solution for a time period necessary for the solution to migrate into the slab. ASTM recommends first sampling at 3 months and subsequent sampling after 6 and 12 months of ponding (ASTM C1543-10a, 2010).

As eluded to above, test methods that directly measure the permeability of a concrete sample are time consuming to perform and thus generally not suitable for quality control (QC) and quality assurance (QA) testing. These test methods become increasingly lengthy in duration when using concretes of higher quality, such as HPC.

2.4 Electrical Methods Used to Indicate Concrete Permeability

Electrical test methods such as the Rapid Chloride Ion Penetrability (RCP) test (ASTM C1202, 2018), surface resistivity (SR), bulk resistivity (BR) and bulk conductivity (BC) are faster to perform by nature, but do not provide a direct measure of concrete permeability. These test methods measure the electrical conductivity or resistance to electricity and are simply indicators of the concretes ability to resist chloride ingress. The correlation of electrical test methods with concrete permeability are based on the pore structure (similar to directly measuring permeability) and the composition of the concretes pore solution. Increased electrical conductivity, and

decreased electrical resistivity, results when more ions are present in the pore solution (Thomas, CE 6503 Course Notes, 2014). The pore solution will not have a direct effect on concrete permeability but will influence the results obtained through electrical testing methods. Shi et al. (1998) noted that the use of SCM's can reduce electrical conductivity of a concrete by up to 90% due to changes in the chemical composition of the pore solution. However, the ease and speed at which electrical testing methods can be performed has still proven to be a very useful tool in QC and QA of concrete materials.

2.4.1 Rapid Chloride Ion Penetration (RCP) Test

In 1977, the Federal Highway Administration (FHWA) contracted Construction Technology Laboratories to develop a method to rapidly determine the permeability of a concrete bridge deck. The original version of the test was developed to be performed in-situ and was developed based on correlations to concrete samples that were ponded with 3% sodium chloride for 90 days as per AASHTO T259. The time required for the field test was considered impractical and the test was thus abandoned for the lab version of the test method, which was adopted by AASHTO in 1983 and as ASTM C1202 in 1991 (Whiting and Mitchell, 1992).

The RCP test is typically carried out over a two-day period. Each of the specimens are sliced to obtain a 50-mm thick portion, coated with epoxy, vacuum saturated for approximately six hours, then placed into the appropriate cells to carry out the testing. One cell is filled with a 3% NaCl solution, while the other was filled with 0.3N NaOH solution. A voltage of 60V is then applied to the sample over a period of 6

hours, and the current passed through the specimen is recorded 30-minute intervals. The total charge passed, $\boldsymbol{Q}$, expressed in coulombs, is calculated by Equation 2.6,

$$\boldsymbol{Q = 900(I_0 + 2I_{30} + 2I_{60} + \ldots + 2I_{330} + I_{360})} \qquad \textbf{Eq. 2.6}$$

where $\boldsymbol{I_0}$ is the current (mA) at time zero (0) when the test is initiated, and $\boldsymbol{I_t}$ is the current (mA) at each 30-minute time interval from time zero until the test finishes at 6 hours or 360 minutes (ASTM C1202, 2018). The basic functionality of the RCP test apparatus is shown in Figure 2.1.

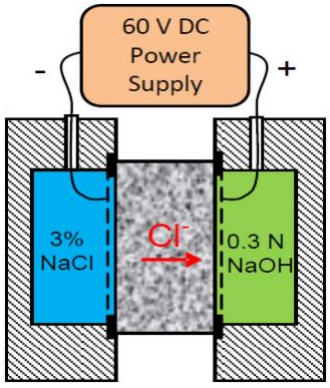

Figure 2.1: RCP Apparatus (Germann Instruments, 2018)

Diffusion coefficients of concrete typically range from $1x10^{-13}$ to $1x10^{-11}$ m^2/s (Thomas, 2013). The correlation of diffusion coefficients obtained from ASTM C1532 to RCP values are shown in Figure 2.2 from Thomas (2013).

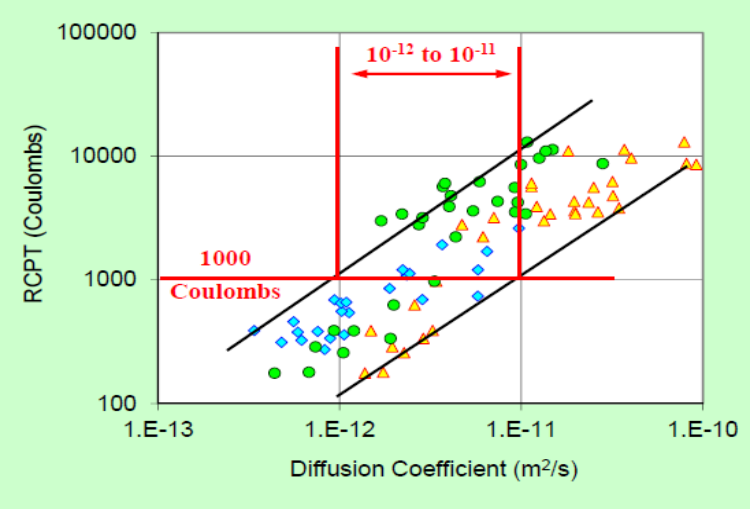

Figure 2.2: RCP vs. Diffusion Coefficient (Thomas, 2013)

Correlations between salt ponding tests and RCP test results hold well for conventional concrete comprised solely of Portland Cement as a binder, but not for concrete containing supplementary cementing materials (SCM's). The use of SCM's result in a change of the composition of the pore structure and pore solution of the concrete. While the composition of the pore solution does not contribute directly to the permeability of concrete, it does influence the measurements obtained when measured with RCP (Shi et al.,1998; Thomas, CE 6503 Course Notes, 2014). Concretes containing SCM's will often indicate a lower RCP reading relative to the results of actual chloride ion penetration results obtained by salt ponding a sample (Nassif et al., 2015).

Criticisms of the RCP test have been made in various reports and research. Nassif et al. (2015) cited the coefficient of variation for RCP tests are 12.3 and 18.0% for interlaboratory and multiple laboratories respectively. In comparison, Icenogle and Rupnow (2011) cited that the coefficient of variation of a single surface resistivity

measurement using a Wenner probe was 6.2%, and 11% for multiple laboratories. Therefore, surface resistivity measurements have been found to be more repeatable.

Another limitation associated with the RCP test is the "Joule Effect", resulting from high current flow through permeable concrete mixes of lesser quality. The Joule Effect is characterized by a rise in sample temperature as high current flows through the sample. This increase in temperature decreases the electrical resistivity of the sample as time passes, effectively increasing the current flow and temperature in a synergistic manner (Ghosh and Tran, 2015).

2.4.2 Electrical Resistivity and Conductivity – Basic Theory

Electrical resistance is a measure of the difficulty in passing an electric current through a material or object under an applied voltage. Resistance can be calculated using Ohm's law in Equation 2.7, where, $\boldsymbol{V}$ is the electrical potential across the sample (volts), $\boldsymbol{I}$ is the current (amps) and, $\boldsymbol{R}$ is the Resistance measured in Ohms (Ω).

$$\boldsymbol{V = I \cdot R} \qquad \textbf{Eq. 2.7}$$

Electrical resistivity is the Resistance, $\boldsymbol{R}$ ($\boldsymbol{\Omega}$), determined from Equation 2.7 above, normalized to a unit cross-section and length (Stanish et al., 1997). Equation 2.8 is used to calculate the electrical resistivity of a material such as concrete, where $\boldsymbol{A}$ is the cross-sectional area of the specimen (m^2), $\boldsymbol{L}$ is the length of the specimen (m) and, $\boldsymbol{\rho}$ is the resulting electrical resistivity (Ω-m).

$$\boldsymbol{\rho = R\left(\frac{A}{L}\right)} \qquad \textbf{Eq. 2.8}$$

Electrical conductivity is the inverse of electrical resistivity as indicated in Equation 2.9, where $\boldsymbol{\sigma}$ is the electrical conductivity measured in Siemens/meter (S/m) and, $\boldsymbol{\rho}$ is the electrical resistivity **(**Ω-m).

$$\boldsymbol{\sigma = \frac{1}{\rho}} \qquad \textbf{Eq. 2.9}$$

2.4.3 Surface Resistivity (SR) Testing

The surface resistivity (SR) of concrete is determined using a 4-point Wenner probe. The Wenner probe was developed by Frank Wenner in 1915 to measure the electrical resistivity of soils, which is a predictor of soil moisture content. In recent years, the Wenner probe has gained in popularity for indicating the permeability of concrete by electrical surface resistivity (SR) measurement (Cook and Van Nostrand, 1966).

The Wenner probe works by passing a current, $\boldsymbol{I}$, through a concrete sample between the two outer probes depicted in Figure 2.3. The electrical potential difference is then measured between the inner two electrodes, obtaining a resistance value using the principles of Ohms law as described earlier. The surface resistivity, $\boldsymbol{\rho}$ (Ω-m), is then calculated from Equation 2.10, where $\boldsymbol{a}$ is the probe spacing (m), $\boldsymbol{V}$ is the measured potential (volts), and $\boldsymbol{I}$ is the current applied to the specimen (mA) (Proceq, 2017).

$$\boldsymbol{\rho = 2\pi a \frac{V}{I}} \qquad \textbf{Eq. 2.10}$$

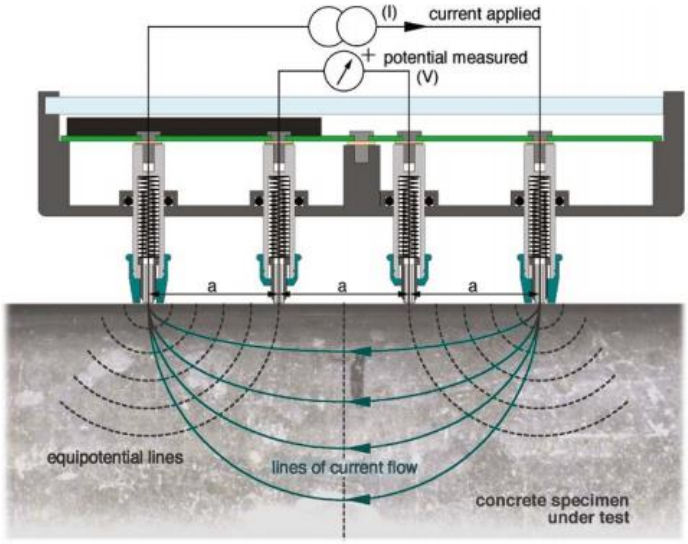

Figure 2.3: Proceq 4-Point Wenner Probe (Proceq, 2017)

Surface resistivity has become a popular method for indicating concrete permeability as the measurements are quick to perform in comparison to the more often used RCP test. The cylindrical samples also require very little preparation prior to testing in comparison to the RCP test where slicing and vacuum saturating are required a day prior to the test. A study sponsored by the New Jersey Department of Transportation (NJDOT) stated as of 2015 that 17 United States highway transportation departments had at least evaluated SR testing as method to indicate concrete permeability. Various transportation departments cite cost reduction and increased repeatability of the test in comparison to RCP as major advantages of the SR test (Nassif et al., 2015; Icenogle and Rupnow, 2011).

Considerations that need to be taken in account when assessing the permeability of concrete using SR is the influence of moisture content, the temperature of the concrete and the influence of geometry (Spragg, et al., 2015). The influences of temperature and moisture content are discussed further in Section 2.5.

Morris et al. (1996) established that the electrical surface resistivity, $\boldsymbol{\rho}$, can be determined using a 4-point Wenner probe with Equation 2.10 presented earlier. However, Equation 2.10 assumes a semi-infinite body of material, which a concrete cylinder or core is not. Therefore, Morris et al. (1996) established cell constant values using finite element simulations associated with various cylinder sizes and typical probe spacing and configurations. Figure 2.4 presents the cell constant correction factor, $\boldsymbol{K}$, determined by Morris et al. (1996) for a 4-point Wenner probe of probe spacing, $\boldsymbol{a}$, centered longitudinally along the cylinders long axis. The resulting surface resistivity, $\boldsymbol{\rho}$, of Equation 2.10 is multiplied by the cell constant value, $\boldsymbol{K}$, to account for the influence in geometry.

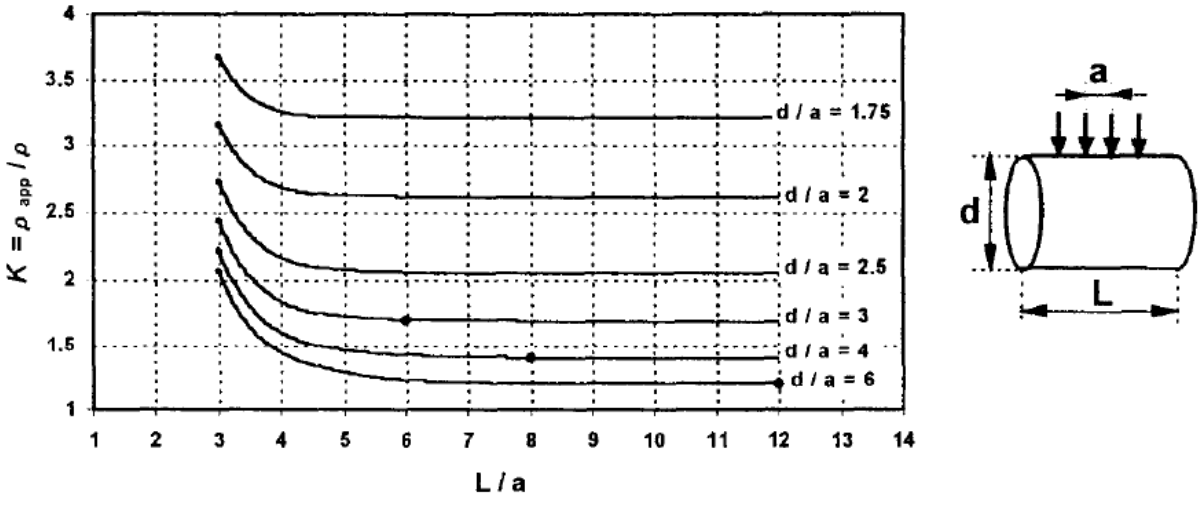

Figure 2.4: Cell Constant Correction Factor (K) Calculation (Morris et al., 1996)

2.4.4 Bulk Resistivity (BR) Testing

The bulk resistivity (BR) of a cylindrical concrete specimen is determined by placing two electrodes on opposite ends of the cylinder and applying an alternating current (AC), $\boldsymbol{I}$ (mA), between the two electrodes. The potential drop, $\boldsymbol{V}$ (volts), is measured by the device, and the impedance, $\boldsymbol{Z}$ (Ω), is calculated using Equation 2.11.

$$\boldsymbol{Z = \frac{V}{I}} \qquad \textbf{Eq. 2.11}$$

Since BR is determined by using alternating current (AC) rather than direct current (DC), the impedance, $\boldsymbol{Z}$, is measured rather than resistance, $\boldsymbol{R}$. Once the impedance, $\boldsymbol{Z}$, is obtained using Equation 2.11, the bulk resistivity (BR) can be calculated using Equation 2.12. In Equation 2.12, $\boldsymbol{\rho}$ is the bulk resistivity (Ω-m), $\boldsymbol{A}$ is the cross-sectional area (m^2) and, $\boldsymbol{L}$ is specimen length (m).

$$\boldsymbol{\rho = \frac{A}{L} Z} \qquad \textbf{Eq. 2.12}$$

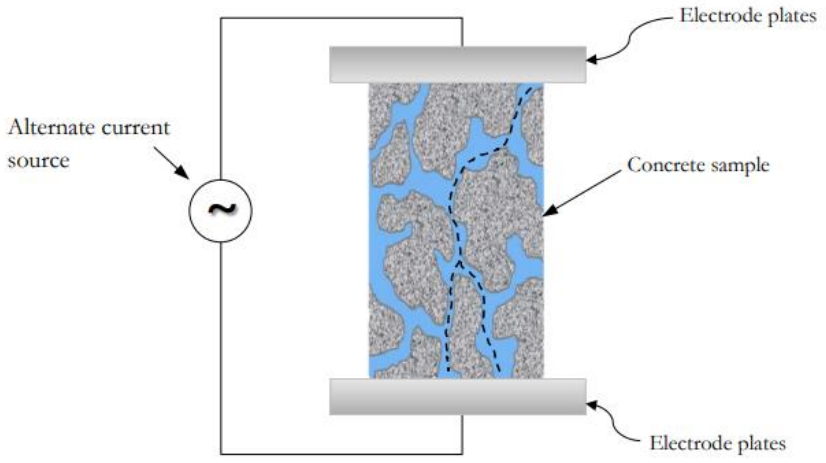

Figure 2.5: Bulk Resistivity Configuration (Giatec Scientific, 2014)

BR testing requires a good electrical contact between the concrete specimen and the electrodes. End grinding of the cylinder ends to create a plane surface free of imperfections and using a conductive medium such as an electrode gel similar to that used in ultrasounds applied to the cylinder ends is required (Spragg et al., 2011).

A distinct disadvantage of the BR test method in comparison to the SR test method using the 4-point probe is that BR test cannot be used to test the electrical resistivity of a concrete element in the field such as a bridge deck or column. An advantage, similar to the SR test, is that the test is rapid to perform and requires minimal specimen preparation other than end grinding.

Similar to SR testing, further considerations that need to be taken in account when assessing the permeability of concrete using BR is the influence of moisture content, the temperature of the concrete and the influence of geometry (Spragg, et al., 2015). However, the geometry factor is known and easily applied to the calculation of BR in Equation 2.12 by dividing the cross-sectional area by the length of the cylinder (Sanchez, 2015).

2.4.5 Bulk Conductivity (BC) Testing

Electrical conductivity is the reciprocal of electrical resistivity as explained earlier. ASTM C1760 is the standardized test method for measuring bulk conductivity (BC) using the same apparatus as used for the RCP test in accordance with ASTM C1202.

Rather than testing a 50-mm slice of a 100-mm diameter concrete cylinder, the full 200-mm length of cylinder is used. The sample is not sealed and both reservoirs are filled with 3% NaCl solution. A 60V charge is then applied to the sample in the same manner as ASTM C1202, however the duration of the bulk conductivity test is 1 minute. Figure 2.6 depicts the basic functionality of the bulk conductivity apparatus.

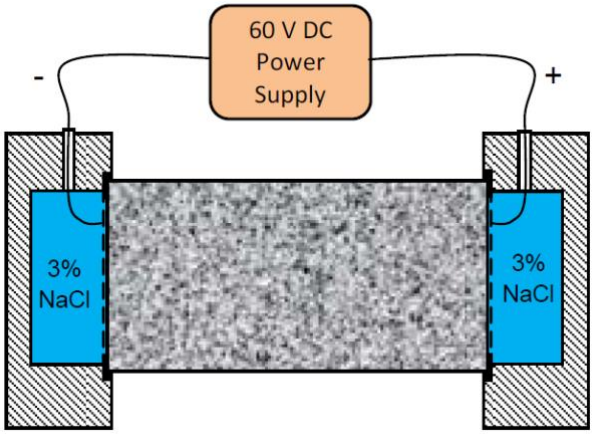

Figure 2.6: Bulk Conductivity Testing Apparatus (Germann Instruments, 2018)

The current, $\boldsymbol{I_1}$ (mA), passing through the specimen at a time interval of 1 minute is used to calculate the bulk conductivity, $\boldsymbol{\sigma}$ (mS/m), of the sample using Equation 2.13. In Equation 2.13, $\boldsymbol{V}$ is the voltage applied to the sample (volts), $\boldsymbol{L}$ is the length of the sample (m), and $\boldsymbol{D}$ is the diameter of the sample (m^2).

$$\boldsymbol{\sigma = 1273.2\ \frac{I_1}{V}\ \frac{L}{D^2}} \qquad \textbf{Eq.2.13}$$

Given that the current, $\boldsymbol{I_1}$, is measured at a time of one minute rather than integrating the current over a time period of 6 hours as is performed in the RCP test, the BC test avoids the concerns of heating of the sample created by the "Joule Effect".

Hooton and Nokken (2006) stated that the initial current from BC testing and the total charge, $\boldsymbol{Q}$, measured coulombs observed over 6 hours were in a linear relationship for concretes with a total charge passed of less than 3000 coulombs. They stated that at greater total charge values above 3000 coulombs obtained from the RCP test, the results of the BC test did not correlate as well because of heating of the sample observed in the RCP test.

Further benefits associated with the BC test is the short one-minute duration to conduct the test, compared to the six-hour timeline for the RCP test that does not include the time it takes to properly prepare the sample. BC testing is also non-destructive to the cylindrical specimen; therefore, the same sample can be used again and again for testing at later ages, similar to SR and BR. The BC test also uses equipment that most concrete testing laboratories already own to perform the RCP test in accordance with ASTM C1202 (Hooton and Nokken, 2006).

2.5 In-Situ Testing of Concrete Using Surface Resistivity (SR)

Isgor and Morales (2015) investigated corrosion inspection of reinforced concrete bridge structures using electrical resistivity. Although corrosion monitoring is not a main topic of this research, common factors such as rebar cover depth, degree of concrete saturation, concrete temperature and rebar spacing were all identified as factors having an effect on SR results when measured using a 4-point Wenner probe. Reinforced concrete slabs consisting of both welded wire mesh and reinforcing steel at 200-mm center to center spacing and at three different cover depths (3.5”, 2.5” and 1.5”) were cast in their study. Measurements were then made using varying 4-point Wenner

probe configurations to identify variations in SR results. Portions of the slabs were cast without any reinforcement and used as a control. It was concluded that additional reinforcing steel depth increases the accuracy of the surface resistivity measurements when concrete is in a semi-saturated or saturated condition. In situations of reduced rebar cover, it is likely that the reinforcing steel will short circuit the induced current from the Wenner probe. It was also concluded that electrical resistivity decreases as corrosion increases, something that is beyond the scope of this study and will not be discussed further.

Isgor and Morales (2015) and Marquez (2015) concluded that electrical resistivity measurements provide more accuracy with increased concrete saturation. This is because the electrical current applied to the specimen is carried through the interconnected pore water, resulting in a measured indication of permeability. A decrease in moisture content will yield higher resistivity results and therefore a false indication of permeability (Marquez, 2015). Figure 2.7, from Marquez (2015), shows that 24 hours is commonly required for saturation to achieve a consistent SR measurement, with more time being required for concretes of lower w/c.

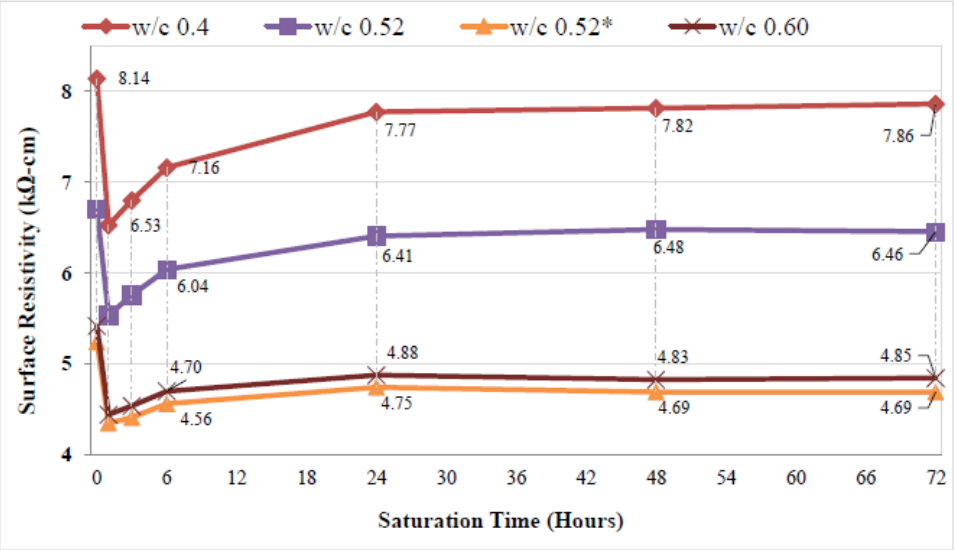

Figure 2.7: Surface Resistivity vs. Saturation Time at 56 Days (Marquez, 2015)

Concrete temperature is also known to have a profound effect on resistivity measurements. Elkey and Sellevold (1995) concluded that for ordinary Portland Cement concrete, resistivity changes approximately 3-5% per 1°C of temperature change, depending on the degree of concrete saturation. A specimen temperature decrease will cause an increase in concrete resistivity. Similarly, a specimen temperature increase will cause a decrease in concrete resistivity (Marquez, 2015).

2.6 Current Specifications and Established SR Threshold Limits

The RCP test is the most widely used electrical test method used on concrete to indicate its permeability. Table 2.1 summarizes the current specifications used to assess concrete permeability using the RCP test as stated in CSA A23.1-14 and the NBDTI Standard Specifications. Note that NBDTI and CSA A23.1 both specify a limit of 1000 Coulombs when testing C-XL concrete with the RCP test, however the age of testing

specified within CSA A23.1-14 is 91 days, whereas NBDTI specified that C-XL concrete meet the 1000 coulomb limit at an age of 56 days.

Table 2.1: RCP Test Limits in CSA A23.1-14 vs. NBDTI

Specifier/Specification	RCP Test Limit (C-XL Concrete)	Age of Testing
CSA A23.1-14	1000 Coulombs	91 Days
NBDTI	1000 Coulombs	56 Days

The New Jersey Department of Transportation (NJDOT) sponsored research performed by the Rutgers Infrastructure Monitoring and Evaluation (RIME) group at the State University of New Jersey to evaluate the surface resistivity (SR) test in accordance with AASHTO TP 95-11 for updating the NJDOT's High Performance Concrete specifications to include a Surface Resistivity (SR) threshold (Nassif et al., 2015). The research was deemed necessary by NJDOT as the research developed by other jurisdictions was not representative of state-specific conditions and different local resources. It was thought that local materials such as aggregates and local cements will create differences in SR threshold limits compared with other jurisdictions in other geographical areas. The SR threshold limits were established to correspond to RCP test results of 1000 and 2000 coulombs (Nassif et al., 2015). Since CSA A23.1-14 and NBDTI use a hard limit of 1000 coulombs for C-XL concrete, only the threshold limits established by RIME and other jurisdictions cited in their report equating to 1000 coulombs will be cited in this study for comparison.

Table 2.2 presents the upper limit threshold SR values implemented in standard specifications by Florida Department of Transportation (FDOT) and Louisiana Department of Transportation (LADOTD) as well as SR threshold values cited in research performed by RIME and AASHTO for quality assurance of High Performance Concrete. These values are intended to equate to a value of 1000 coulombs when using the SR test to compare to the more established RCP test. The variance between the threshold values for SR testing established by each organization as shown in Table 2.2 does reinforce the need for testing with local materials to establish threshold limits for SR values to be used in specifications where concrete acceptance and payment adjustments for SR test results may be applied to contract unit prices for concrete placed in a structure.

Table 2.2: Surface Resistivity Threshold Value for HPC by Jurisdiction (Adopted from Nassif et al., 2015)

Jurisdiction / Organization	**RIME**	**NJDOT**	**AASHTO**	**Louisiana DOT**
Threshold SR Value (*Equal to 1000 C*) – 56 Days	**48kΩ-cm**	**43kΩ-cm**	**37kΩ-cm**	**37kΩ-cm**

3 EXPERIMENTAL DETAILS

3.1 Equipment

3.1.1 Rapid Chloride Ion Penetration (RCP) Testing (ASTM C1202)

The Proove'it device by Germann Instruments was used for the RCP testing. Two different machines at two separate laboratories were used for this portion of the study. Samples cast in the field, on NBDTI project sites, were sent to a local Canadian Council of Independent Laboratories (CCIL) certified laboratory for testing as per an existing contract with NBDTI. Samples that were cast in the lab were tested for RCP at the University of New Brunswick (UNB) using the same model of device.

In this test method, a 50-mm slice was cut from each cylinder and used for the test. The reservoir with the negative (-) connection is filled with 3% NaCl solution, while the reservoir with the positive (+) connection is filled with 0.3N NaOH solution.

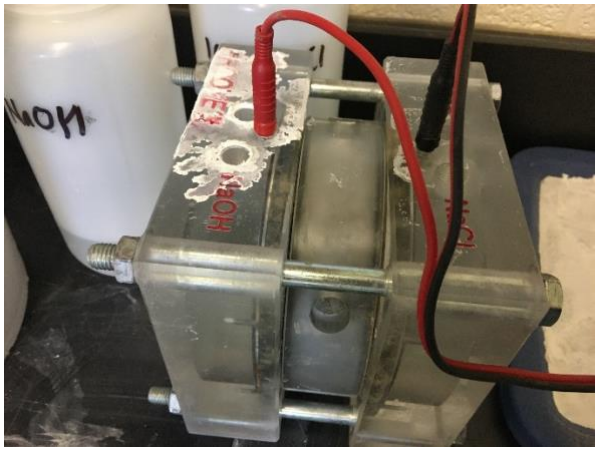

Figure 3.1: Proove'it RCP Apparatus at UNB

3.1.2 Surface Resistivity (SR) Testing

The Resipod 4-point Wenner probe, manufactured by Proceq, equipped with a 38-mm probe spacing as shown in Figure 3.2 was used in this study for the purpose of measuring surface resistivity.

(a) **(b)**

Figure 3.2: (a) and (b), Resipod 4-point Wenner Probe by Proceq. Equipped with 38mm Probe Spacing

3.1.3 Bulk Resistivity (BR) Testing

The RCON device shown in Figure 3.3, developed and manufactured by Giatec Scientific, was used to test for bulk resistivity (BR) throughout this study. The cylinder ends were treated with Spectra 360 electrode gel prior to testing.

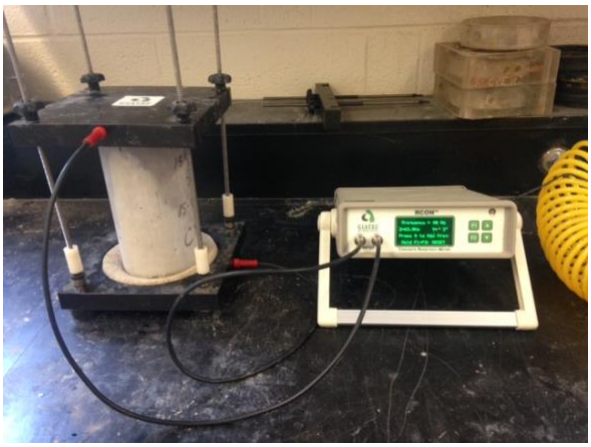

Figure 3.3: RCON device in use at UNB lab

3.1.4 Bulk Conductivity (BC) Testing (ASTM C1760)

The Proove'it device by Germann Instruments was used to carry out the bulk conductivity testing for this study. The apparatus is the same as that used for RCP testing in accordance with ASTM C1202. Rather than testing a 50-mm slice of a 100-mm diameter concrete cylinder, the full 200-mm length of cylinder is used. The sample is not sealed and both reservoirs are filled with 3% NaCl solution. A 60V charge is then applied to the sample in the same manner as ASTM C1202, however the duration of the bulk conductivity test is 1 minute. Figure 3.4 depicts the basic functionality of the bulk conductivity apparatus.

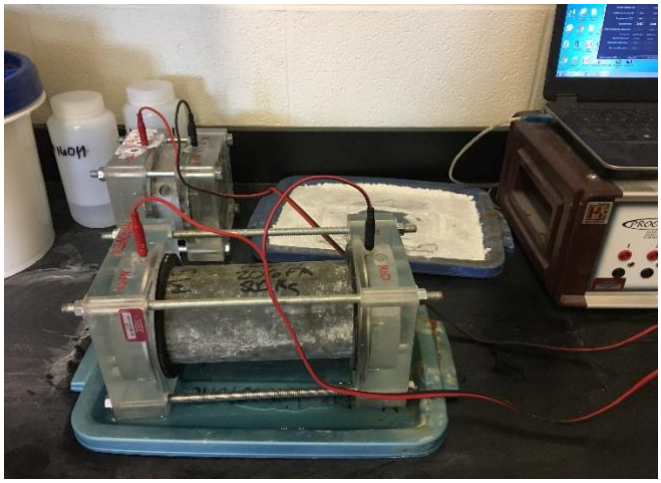

Figure 3.4: Bulk Conductivity Test Using Proove'it Device at UNB

3.2 Mixture Proportions

Concrete mix designs P1 to P13 consisted of samples taken from NBDTI project sites. All of the mixes taken from NBDTI project sites were designed to meet the requirements for exposure class C-XL as summarized in Table 1.1, with the exception of P11 and P12 which were mixes used for curb and gutter and a concrete element of C-1 exposure respectively. As most of the mixes are of the same exposure class and designed to meet the same specification, they contain similar proportions of materials. Also, some mixes were produced by the same concrete supplier. The basic composition of each mix design is presented in Table 3.1.

Given the similarity of the concrete mixes taken from NBDTI project sites (11 out of 13 meeting C-XL exposure specifications), 6 lab mixes were produced at the UNB lab to broaden the range of concrete mixes tested in this study. Lab mixes are noted as L1 to L6 in Table 3.1.

Table 3.1: Concrete Mix Designs (Field and Lab) Used in Study

Mix ID	Cementitious Content (kg/m3)	W/CM	Silica Fume (%)	Fly Ash (%)	Slag (%)	Sand (kg/m3)	Stone (kg/m3)	Nominal Stone Size
P1	430	0.38	5.6	20	-	642	1022	19mm
P2	420	0.37	4.7	7	23	704	1024	19mm
P3	480	0.31	4.8	5	24	663	1029	19mm
P4	489	0.36	6.4	20	-	644	1072	19mm
P5	430	0.38	5.6	20	-	671	991	19mm
P6	430	0.38	5.6	20	-	659	1022	19mm
P7	420	0.38	4.6	7	23	712	1017	19mm
P8	450	0.38	6	25	-	Proprietary	Proprietary	14mm
P9	420	0.38	4.6	7	23	712	1017	19mm
P10	450	0.34	5	25	-	673	1060	19mm
P11	350	0.45	-	-	-	710	1015	19mm
P12	400	0.40	-	20	-	925	960	14mm
P13	510	0.40	4.1	20.6		600	1000	19mm
L1	400	0.45	-	-	-	730	1050	19mm
L2	400	0.55	-	-	-	730	1050	19mm
L3	400	0.45	-	10	-	730	1050	19mm
L4	400	0.45	-	5	-	730	1050	19mm
L5	450	0.40	5	20	-	730	1050	19mm
L6	500	0.34	10	25	-	730	1050	19mm

For the NBDTI project mixes (P1-P13), all coarse and fine aggregates utilized in each mix design are tested on an annual basis to ensure they meet the physical and chemical requirements of CSA A23.1-14. NBDTI specifies more stringent criteria for AAR and micro-deval testing that each aggregate type must satisfy in addition to the requirements of CSA A23.1-14. The stone size of each mix ranged from 14-mm to 19-mm, as noted in Table 3.1.

Given the permeability requirements of type C-XL concrete, supplementary cementing materials (SCM's) must be utilized in each project mix design to meet the specification. Slag was utilized in 4 of the mix designs as a portion of a tertiary blended Portland Cement. Fly ash was utilized in all mixes with the exception of P11, L1 and L2. The majority of concrete mix designs for NBDTI bridge structures use Type F Fly Ash as it is the most available SCM in this region. All fly ashes meet the CSA A3000 requirements for Type F. Silica Fume was utilized in 13 of the 19 mixes. All the silica

fume used, with the exception of P2, P3, P7 and P9 was a bagged silica fume produced by Master Builders (MasterLife 100). All other silica fume sources were part of a blended cement. It should also be noted that while mixes P7 and P9 were the same, they were from two separate NBDTI bridge projects.

All of the concrete samples taken from NBDTI projects (with the exception of P11 and P12) were of exposure class C-XL, designed to meet the 1000 coulomb limit associated with RCP testing at an age of 56 days (NBDTI specifies C-XL concrete to meet a 1000 coulomb limit at 56 days versus 91 days as now specified in CSA A23.1-14). Thus, a combination of silica fume and fly ash is regularly used. Silica fume comes in two forms; as a component of a blended cement or as a separate material added to the ready-mix truck by bags as some plants in the region do not have a second silo available to carry a blended cement in addition to their typical General Use (GU) Portland cement.

Total cementitious contents ranged from 420 to 489 kg/m^3. The Portland cement portion of each mix, whether a blended cement or not, was of type GU. Portland Limestone Cement (Type GUL), although utilized on other NBDTI projects, was not incorporated in any of the mix designs used for this study.

Each lab mix was produced in the UNB laboratory using similar materials in different proportions. The GU cement used was Lafarge's Paulding, Ohio source. The fly ash was Type F from Belledune, New Brunswick. The silica fume was the Master Builders product, MasterLife 100. The details of each mix are presented in Table 3.1. Further details regarding the casting of lab mixes is presented in Section 3.3.

3.3 Casting, Curing and Testing

3.3.1 Casting

Concrete samples from 13 separate NBDTI projects were cast for this study. Concrete samples were of standard 100-mm diameter by 200-mm height cylinders and cast on each job site by a CSA Field Testing - Grade 1 certified technician. NBDTI typically casts multiple cylinders per placement to conduct tests such as compressive strength, hardened air void analysis and RCP testing. Additional cylinders were cast for resistivity as companions to the cylinders cast for RCP testing for this study.

Each concrete cylinder was cast using the CSA A23.2-3C procedure, filling each mold in three lifts and rodding each layer 20 times for a slump less than 180mm and 8 times for a slump greater than 180mm. A metal 10mm diameter hemispherical tipped rod was used to consolidate each layer. Each layer was then tapped smartly 8-10 times before proceeding with the next layer.

All concrete was sampled between 10% and 90% portions of a randomly selected load on site as per the normal requirements of NBDTI's Quality Assurance specifications and CSA A23.2-1C.

Concrete samples taken from 11 of 13 NBDTI projects were of exposure class C-XL, thus most of the concrete samples yield similar results for RCP and resistivity testing within a certain degree of variability as the mix designs are somewhat similar. To broaden the results of this study, 6 lab mixes were produced to mix designs detailed in Table 3.1 and discussed briefly in Section 3.2.

Each lab mix (L1-L6) was produced in the UNB lab in a 20L rotary pan mixer to a target slump of 180-mm by utilizing Master Glenium 7700 polycarboxylate superplasticizer. Addition rates of superplasticizer ranged from 30ml to 70ml. Lab mix 6 required the highest addition of superplasticizer, 70mL, to achieve the target slump.

Cylinders were cast in the laboratory by filling each 100mm diameter mold in three lifts, rodding each layer 8 times (20 times if slump was less than 180mm) with a metal 10mm diameter hemispherical tip rod and tapping smartly 8-10 times until all voids in each layer were filled.

3.3.2 Curing

All concrete cylinders were stored on site for the first 20 to 36 hours in a container capable of maintaining temperature between 15 and 25 degrees Celsius. These containers varied depending on the ambient conditions that the concrete was placed in. In warmer temperatures, an open-air plastic tote filled with water to maintain the temperature in the range noted above was typically used. As temperatures became colder, generally starting late September, an insulated wooden box with a light bulb heating source was used for the initial storage of concrete cylinders. Variations within the temperature range for initial specimen storage is normal and is a function of the ambient temperature and type of curing box used at the job site. All samples were then transported to a regional NBDTI lab for storage under final curing conditions as per CSA A23.2-3C (2014). A summary of projects, regional laboratories and a description of the laboratory curing conditions is presented in Table 3.2.

In the case of the lab cast concrete cylinders at UNB, the cylinders were left to cure on the floor under wet burlap and plastic for the first 24 hours. After 24 hours, each cylinder mold was removed and the cylinders were stored in the UNB moist curing room until the time of testing.

Table 3.2: Curing Regime by Project/Lab Mix

Project ID	Regional Lab	Curing Condition
P1	Fredericton Central Lab	Moist Curing Room (21-25°C)
P2	Renforth Regional Lab	Lime Saturated Water (21-25°C)
P3	Moncton Regional Lab	Lime Saturated Water (21-25°C)
P4	Bathurst Regional Lab	Lime Saturated Water (21-25°C)
P5	Fredericton Central Lab	Moist Curing Room (21-25°C)
P6	Fredericton Central Lab	Moist Curing Room (21-25°C)
P7	Moncton Regional Lab	Lime Saturated Water (21-25°C)
P8	Fredericton Central Lab	Moist Curing Room (21-25°C)
P9	Moncton Regional Lab	Lime Saturated Water (21-25°C)
P10	Rexton Regional Lab	Lime Saturated Water (21-25°C)
P11	Moncton Regional Lab	Lime Saturated Water (21-25°C)
P12	Fredericton Central Lab	Moist Curing Room (21-25°C)
P13	Moncton Regional Lab	Lime Saturated Water (21-25°C)
L1 – L6	UNB Lab	Moist Curing Room (21-25°C)

3.3.3 Sample Preparation

All testing for RCP and resistivity took place in Fredericton, therefore all cylinders then had to be transported from their regional laboratories to Fredericton (if they were not already stored at the Fredericton Central Lab). The cylinders to be tested for RCP were delivered to a local certified laboratory as per the existing NBDTI contract, and all resistivity cylinders were delivered to the Fredericton Central Lab. During transportation, all cylinders were kept in sealed plastic bags to prevent moisture loss. Transportation times did not exceed four hours. Cylinders tested for resistivity were finally transported from the Fredericton Central Lab to UNB in sealed plastic bags for testing typically 1 to 2 days prior to scheduled testing.

Prior to performing any resistivity and conductivity testing at the UNB lab, all cylinders were put into an end grinder to achieve a plane uniform surface profile for testing. Figure 3.5 displays three 100-mm diameter cylinders which have already had one side ground to achieve a uniform surface profile. This method also eliminates the need for sulfur capping when cylinders are to be tested for compressive strength, however compressive strengths were not tested in this study.

Figure 3.5: Concrete Cylinders in End Grinder

End grinding of the concrete cylinders took place days prior to testing; therefore, the cylinders were returned to the moist room at UNB after grinding was complete. At an age of 56 days, the cylinders were removed from the moist curing room and expeditiously tested for SR, BR and BC.

3.3.4 Rapid Chloride Ion Penetrability (RCP) Test (ASTM C1202)

All concrete specimens tested in accordance with ASTM C1202 for Rapid Chloride Ion Penetrability were delivered to an independent laboratory in Fredericton between 7 and 56 days. As was the case with the transportation of all other cylinders, each was placed in a sealed plastic bag and the time of transportation did not exceed four hours. Upon arrival at the independent laboratory, each was placed in a lime saturated water curing tank, meeting the temperature requirements of CSA A23.2-2C and presented in Table 3.2.

The testing process for ASTM C1202 was typically carried out over a two-day period. Each of the specimens were sliced to obtain a 50-mm thick portion, coated with epoxy, vacuum saturated for approximately six hours, then placed into the appropriate cells to carry out the testing (Note – UNB apparatus contains a plastic sleeve to seal specimen, eliminating the use of the epoxy). One cell was filled with a 3% NaCl solution, while the other was filled with 0.3N NaOH solution. A voltage of 60V was then applied to the sample over a period of 6 hours, recording the current passed through the specimen at 30-minute intervals. The total charge passed ($\boldsymbol{Q}$), expressed in coulombs, was then calculated by Equation 2.6 in Section 2.4.1.

The diameter of the cylinder molds used to cast concrete cylinders for this study were 4-inch (100-mm), whereas the ASTM C1202 standard applies to a 3.75-inch (95-mm) diameter specimen. Therefore, the cumulative charge passed through each 4inch (100-mm) specimen was required to be factored to equate to a 3.75-inch diameter specimen using the Equation 3.1,

$$\boldsymbol{Q_s = Q_x * \left(\frac{3.75}{x}\right)^2} \qquad \textbf{Eq. 3.1}$$

where $\boldsymbol{Q_s}$ is the charge passed through a 3.75-inch diameter specimen, $\boldsymbol{Q_x}$ charge passed through an $\boldsymbol{x}$ diameter specimen (inches) (ASTM C1202, 2018).

3.3.5 Surface Resistivity (SR) Testing

The Resipod by Proceq, equipped with 38-mm probe spacing, was used to test for surface resistivity (SR). AASTHTO TP 95-14 was used as the basis for the lab testing procedure for SR testing, with two exceptions: 1) the test results of lime water

cured samples were not multiplied by a factor of 1.1, and 2) a frequency of 40Hz was applied to each sample, rather than 13Hz as prescribed in the test method.

Four marks oriented 90 degrees apart, were placed on each cylinder specimen. Four lines were then marked parallel to the longitudinal axis and aligned with each of the four end marks. The center of each longitudinal line was marked as well to identify the longitudinal center of the specimen when testing. Figure 3.6 depicts an example of the markings of each cylinder.

Figure 3.6: Cylinders Marked at 90 Degree Intervals in Preparation for SR Testing

Prior to each test, the Resipod probes were submerged and pressed into water to apply a conductive fluid to the probe. The probe was then tested for calibration on the test strip provided in the Proceq kit. The cylinders were tested by taking eight measurements, two at each of the lines marked on the cylinder and averaged to obtain a final value as per the specified procedure in AASHTO TP 95-14. The Resipod probe measure SR directly in units of kΩ-cm. After the SR measurements were taken directly

from the 4-Point Wenner probe, the result multiplied by the cell correction factor, $\boldsymbol{K}$, established from Figure 2.4. Equation 2.10 as presented in Section 2.4.3 becomes Equation 3.2, where $\boldsymbol{\rho}$ is the surface resistivity corrected for geometry (kΩ-cm), $\boldsymbol{V}$ is the voltage measured potential (volts), $\boldsymbol{I}$ is the current applied to the specimen (mA), and $\boldsymbol{K}$ is the cell constant correction factor derived from Figure 2.4 (1.95).

$$\boldsymbol{\rho = 2\pi a \frac{V}{I} * K} \qquad \textbf{Eq. 3.2}$$

It should be noted that AASHTO TP 95-14 has now been superseded by AASHTO T 358.

3.3.6 Bulk Resistivity (BR) Testing

Following the tests for surface resistivity, the cylinders were tested for bulk resistivity with the guidance of ASTM test method that was in development at the time the majority of the testing was performed; Draft #7, dated June 12, 2015. Bulk resistivity measurements were performed with a Giatec RCON device, produced by Giatec Scientific Inc., as detailed in Section 3.1.3.

Spectra 360 electrode gel was applied to each end of the specimen to provide a uniform conductive surface prior to placing specimens in the testing apparatus. The specimens were tested at an applied frequency of 40Hz, the same frequency applied by the Resipod probe for consistency. The value of impedance, $\boldsymbol{Z}$, was obtained by the device and then used to calculate bulk resistivity by using Equation 2.12 presented in Section 2.4.4.

3.3.7 Bulk Conductivity (BC) Testing

Bulk Conductivity testing was performed in accordance with ASTM C1760. During the setup of the testing cells, the specimens were kept moist by applying a wet towel to prevent moisture loss as shown in Figure 3.7(a). Care was taken not to spill any sodium chloride (NaCl) on the concrete specimens, as this would have artificially increased measurements and falsely indicate poor concrete. The current, $\boldsymbol{I_1}$ (mA), passing through the specimen at a time interval of 1 minute was used to calculate the bulk conductivity, $\boldsymbol{\sigma}$ (mS/m), using Equation 2.13 presented in Section 2.4.5.

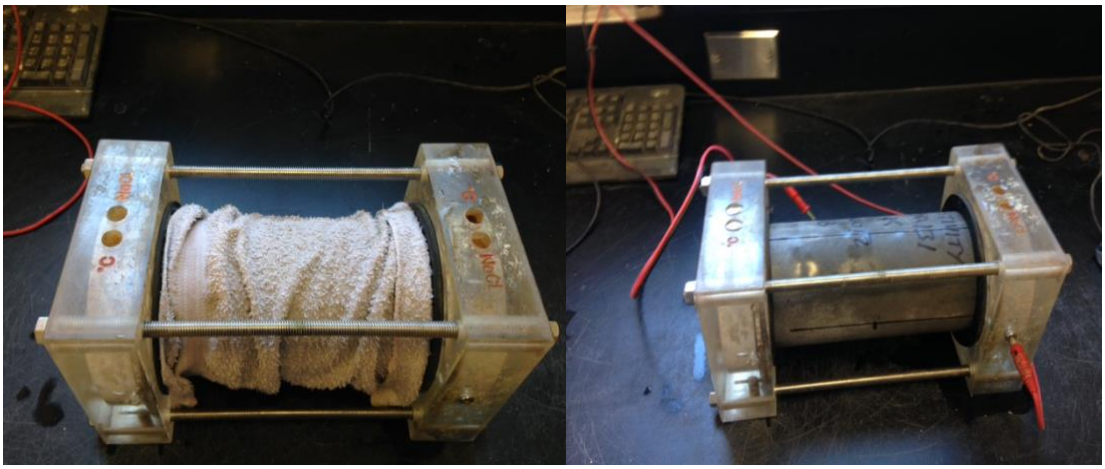

(a) **(b)**

Figure 3.7: (a), Concrete Sample Covered in Moist Cloth Awaiting Testing, (b), Concrete Sample Being Tested for Bulk Conductivity

Since the bulk conductivity testing was carried out on a device separate from the RCON which was used in determining BR, the reciprocal of the bulk conductivity was calculated to represent bulk resistivity of each sample for comparison to the other test methods. Equation 3.3 shows the relationship of bulk conductivity to bulk resistivity

discussed in Section 2. In Equation 3.1, $\boldsymbol{\rho}$ is the bulk resistivity (kΩ-cm), $\boldsymbol{V}$ is the applied voltage to the sample (volts), $\boldsymbol{I}$ is the current obtained at 1 minute (mA), $\boldsymbol{L}$ is the length of the sample (cm), and $\boldsymbol{d}$ is the diameter if the sample is (cm^2) (Thomas, CE 6503 Course Notes, 2014).

$$\boldsymbol{\rho = \left(\frac{V}{I}\right)\left(\frac{\pi d^2}{4L}\right) = \frac{1}{\sigma}} \qquad \textbf{Eq. 3.3}$$

As stated in Section 3.2.4, the bulk conductivity test uses the same apparatus and overall principles as the RCP test. Therefore, it is possible to calculate the predicted charge, $\boldsymbol{Q}$ (coulombs), at 6 hours, based on the current obtained after 1 minute with the larger specimen (200-mm length vs. 50-mm length). Equation 3.4 was used to predict the charge passed at a duration of 6 hours in coulombs (similar to ASTM C1202).

$$\boldsymbol{Q = \frac{\left[\left(\frac{V_{200mm\ Length}}{V_{50mm\ Length}}\right)\ x\ I_1\ x\ 21600\right]}{1000}} \qquad \textbf{Eq. 3.4}$$

In Equation 3.4, $\boldsymbol{V_{200mm\ Length}}$ represents the volume of the full size (200-mm length) sample, and $\boldsymbol{V_{50mm\ Length}}$ represents the volume of the 50-mm slice that is used for the RCP test. $\boldsymbol{I_1}$ represents the current obtained from the device at 1 minute. The concept of this equation was developed from Hooton and Nokken (2006). These results were then compared to the values for total charge, $\boldsymbol{Q}$, obtained using the RCP test and are presented in Section 4.3.

3.3.8 In-Situ Testing

To begin to evaluate the possibility of using surface resistivity testing to evaluate concrete as placed in the field, measurements were taken on concrete placed in three

newly built structures at an age of 56 days and compared to cylinders taken from the same concrete and cured under lab conditions. The depth of concrete cover was designed for 60-mm to 70-mm and verified by inspection in the field prior to placing concrete.

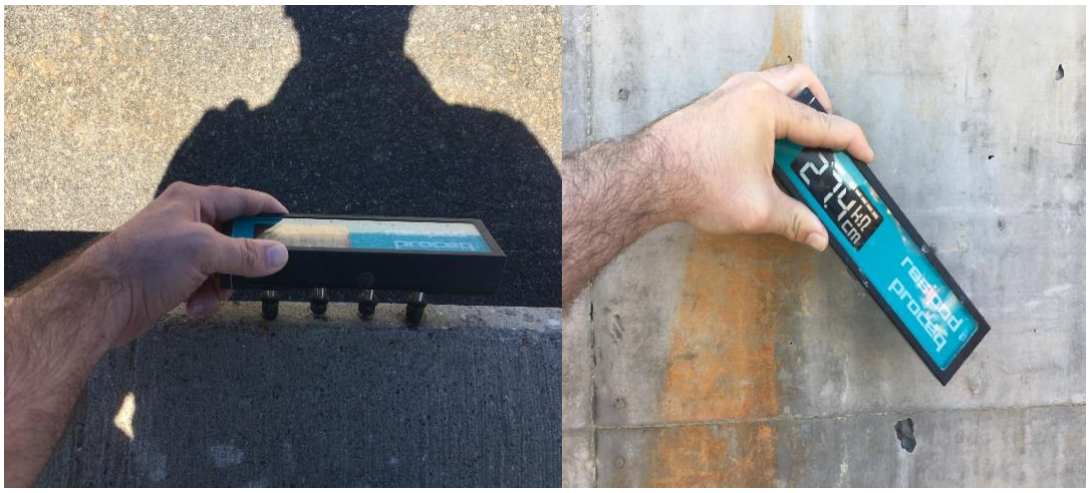

(a) **(b)**

Figure 3.8: (a), SR Field Measurement Along Chamfered Edge of Sidewalk (P1), (b), SR Field Measurement Diagonal to Reinforcing Steel (P13)

Prior to taking any measurements, the probes of the Wenner device were saturated with water in a plastic container. Measurements with the Wenner probe were taken in primarily perpendicular orientation to the reinforcing steel as is recommended by the Resipod brochure by Proceq.

The temperature of the concrete surface was taken using a standard infrared temperature gun. Further discussion is undertaken in the next section.

3.4 Effect of Varying Temperature on Surface Resistivity

To determine the effect of surface temperature on surface resistivity measurements, specimens from lab mixes 2 and 4 were subjected to five separate temperatures ranging from -18°C to 60°C. All samples were an age of 58 days when tested. Table 3.3 details how each temperature treatment was obtained.

Table 3.3: Methods of Temperature Treatment for Determination of Temperature Effect on Surface Resistivity

Temperature	Method
-18°C	Deep Freezer
-2°C	Mini Refrigerator
23°C	Room Temp
38°C	Cooled from Hot Water Bath
60°C	Hot Water Bath

The hot water bath utilized to subject concrete samples to a 60°C temperature was the same apparatus used by NBDTI to perform asphalt testing at their central laboratory in Fredericton. Each sample remained in the bath for 24 hours to ensure saturation prior to testing. Measurements made at 38°C were simply performed on the same cylinders subjected to cooling at room temperature until it reached a temperature of 38°C as measured by an infrared temperature gun.

Temperature treatments of -2°C and -18°C were obtained by a home mini fridge and deep freezer respectively, as noted in Table 3.3. Each sample was saturated in a 5-gallon pail using municipal tap water prior to sealing in plastic bags as shown in Figures

3.9 and 3.10. Each specimen remained in its respective temperature environment for approximately 12 hours prior to testing. A digital stem thermometer in combination with an infrared temperature gun were used to confirm the surface temperatures of the samples at the time of testing. Due to the 12-hour immersion time in each temperature treatment, it was determined that obtaining the surface temperature of each specimen would represent the bulk temperature of the sample.

(a) **(b)**

Figure 3.9: (a), 60°C Water Bath, (b), Sealed Concrete Cylinders in Mini-Fridge at -2°C

(a) **(b)**

Figure 3.10: (a), Two Sealed Cylinders immediately After removal From Freezer, (b), Cylinders at -18°C After Removal From Sealed Bags

4 RESULTS AND DISCUSSION

4.1 Sample Preparation and Curing

All the data and results for surface resistivity (SR), bulk resistivity (BR), bulk conductivity (BC) and rapid chloride ion penetrability (RCP) are tabulated in Appendix A to D respectively.

Since all samples from the NBDTI projects were cast in field conditions, using multiple technicians and multiple curing lab locations across the province, it is necessary to expect some variance in the data. However, the purpose of this study was to investigate the viability of using various electrical resistivity measuring techniques as a possible supplement or replacement to the RCP test that is currently specified by NBDTI to evaluate the performance of cast in place concrete. Therefore, despite possible discrepancies, it is important that this study be performed using field cast specimens.

It should be noted that a mixture of lime saturated curing tanks and moist curing rooms were used at various stages of the curing life, between 1 and 56 days, prior to testing. Hamilton III et al. (2007) and Nassif et al. (2015) compared the numerical difference in SR between cylinders cured in lime water to those cured in a room at 100% relative humidity. It is stated that in terms of curing regime, there was a negligible difference in SR when specimens were cured for more than 28 days in either 100% humidity or immersed in lime water at 23 degrees Celsius. Therefore, the possible variance in curing regimes for different projects, which was largely dependent on the

region of the province the project was located and the equipment available in the regional lab, was largely ignored for this study.

4.2 Surface Resistivity and Bulk Resistivity vs. ASTM C1202

As per the research established by Morris et al. (1996), detailed in Section 2.4.3, each surface resistivity measurement was corrected by a cell constant correction factor, K. A factor of 1.95 was determined from Figure 2.4.

Previous studies have been used to correlate the data taken for SR to data obtained by ASTM C1202. Studies from the Rutgers Information Monitoring and Evaluation Group (RIME), New Jersey Department of Transportation (NJDOT), Louisiana Department of Transportation and Development (LADOTD), and AASHTO were obtained from research conducted by the RIME Group (Nassif et al., 2015). Figure 4.1 depicts the line of best fit for each of the respecting data series mentioned above, as well as the data and line of best fit for SR and BR data taken during this study (UNB Data).

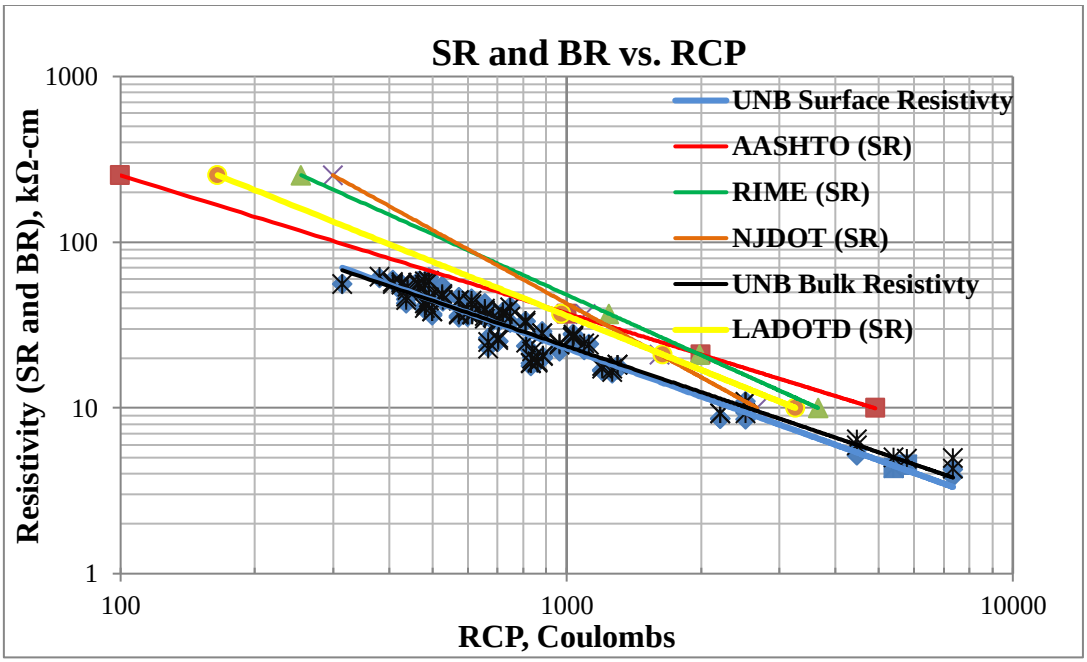

Figure 4.1: SR and BR vs. RCP. Data Included from AASHTO, RIME, LADOTD and NJDOT (Adopted from Nassif et al., 2015)

The data obtained in this study at UNB correlates reasonably well to the data obtained by the other transportation jurisdictions and research bodies, although the UNB data set does tend to show lower resistivity values for each corresponding RCP value when compared to the other data sets. Threshold values for C-XL concrete, using the equations developed from both the bulk resistivity and surface resistivity data, yield threshold values of 23.5 kΩ-cm and 22.9 kΩ-cm respectively when equating to 1000 coulombs of charge. These are significantly lower values than those indicated in Table 2.2 for RIME, NJDOT, AASHTO and LADOTD.

It should be noted that all but four (4) of the C-XL concrete samples obtained from NBDTI project sites contained 15L/m^3 of calcium nitrite corrosion inhibitor (CNI). Calcium nitrite is known to decrease resistivity and therefore increase the electrical

conductivity of a concrete sample (Nassif et al., 2015; ASTM C1202, 2018). Therefore, the resulting decrease in electrical resistivity results in a relative increase in the total charge passed during the RCP test and can largely be ignored when comparing this data to that of other jurisdictions without a corresponding direct permeability measurement such as ASTM C1556 or ASTM C1543.

Results for SR and BR obtained during this study on the same samples correlate very well, after SR measurements are corrected by a K factor of 1.95. Figure 4.2 shows SR vs. BR measurements taken during this study. The $R^2 = 0.9841$, representing a very well correlated data set of results. Given the good correlation of results, the K factor of 1.95, obtained from Morris et al. (1996), appears to be valid.

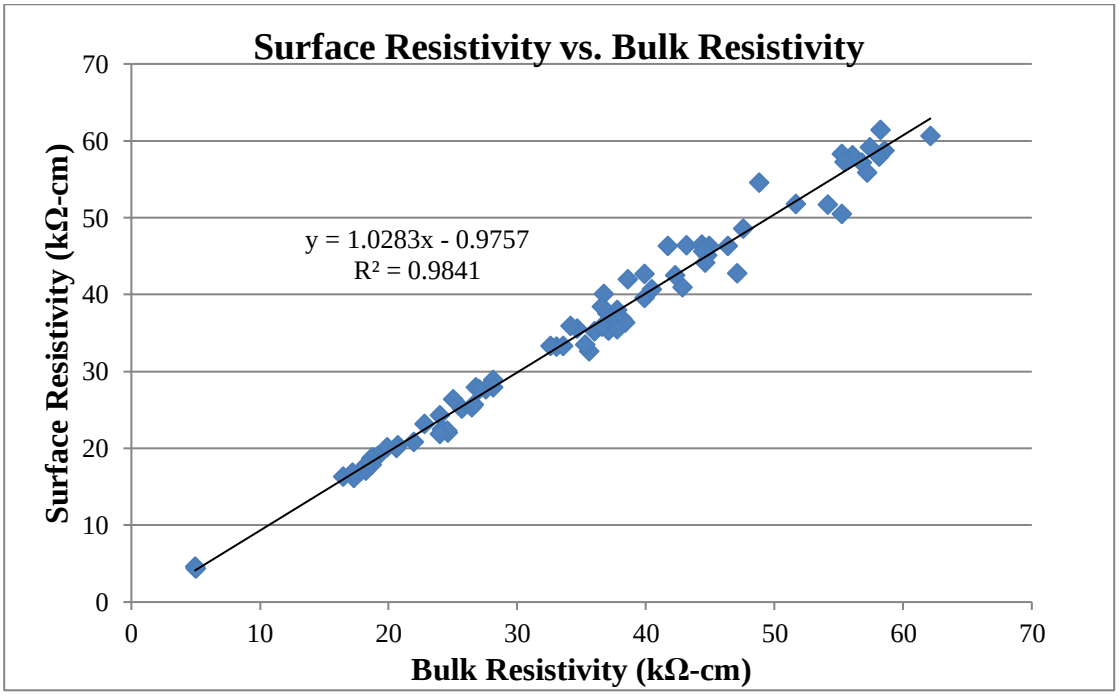

Figure 4.2: Bulk Resistivity (RCON) vs. Surface Resistivity (Proceq Resipod 4-Point Wenner Probe)

4.3 Bulk Conductivity Testing

Bulk conductivity testing, in accordance with ASTM 1760, was evaluated in comparison to bulk resistivity data obtained using the RCON. The current obtained at a time of 1 minute, $\boldsymbol{I_1}$, was used in Equation 3.3 to calculate the resistivity from the data obtained by the bulk conductivity test. Equation 3.3 calculates resistivity by using the reciprocal of bulk conductivity ($\boldsymbol{\sigma}$). Figure 4.3 displays the measurements obtained for bulk resistivity using the RCON device versus the reciprocal of the bulk conductivity ($\boldsymbol{\sigma}$) values obtained by ASTM C1760. The data correlates well with an $R^2 = 0.9397$. Five data points were removed from the graphed dataset due to abnormally high values obtained for the current (mA) at 1 minute when testing for bulk conductivity when comparing to companion cylinders. These abnormally high values for current were typically obtained when NaCl solution leaked from the cells onto the surface of the cylindrical specimen.

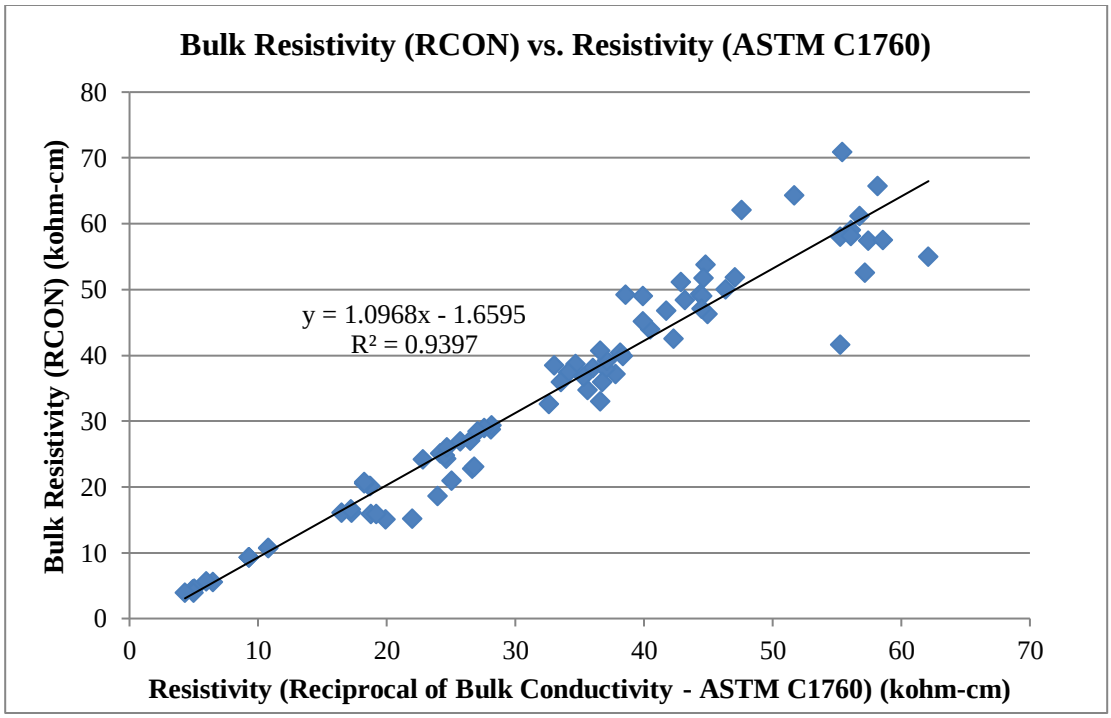

Figure 4.3: Bulk Resistivity (RCON) vs. Resistivity from ASTM C1760

As discussed in Section 2.4.1, two of the limitations of the RCP test are the "Joule Effect", whereby the sample temperature rises as the test progresses and increases electrical conductivity, and the approximately two days necessary to prepare and test samples after they have been properly cured (Ghosh and Tran, 2015). The Bulk Conductivity test was utilized to determine the charge passed through a 200-mm length of concrete at 1 minute and predict the charge passed through the same concrete of 50-mm length over a 6-hour period using Equation 3.4. This technique reduces the test time significantly from a 2-day period to merely minutes and eliminates the concern with temperature rise and increased electrical conductivity as the test progresses, thus avoiding erroneously high conductivity results. This version of the test is also non-

destructive, allowing the same sample to be tested continuously over time or to be utilized for other test methods (Hooton and Nokken, 2006).

The predicted charge of each sample tested using bulk conductivity versus its companion cylinder tested for RCP are displayed in Figure 4.4. A good correlation between the results is found ($R^2 = 0.9456$), however variations in the companion results do exist as shown in Figure 4.5. Hooton and Nokken (2006) noted that a linear relationship exists between the results of BC and RCP testing until an RCP value of 3000 coulombs, after which there is a divergence due to the heating of the sample. The data presented in Figure 4.4 does not tend to fully support this claim, however only 6 specimens cast tested at an RCP value exceeding 3000 coulombs, making it difficult to accurately comment on the claim presented by Hooton and Nokken (2016) with such a limited data set.

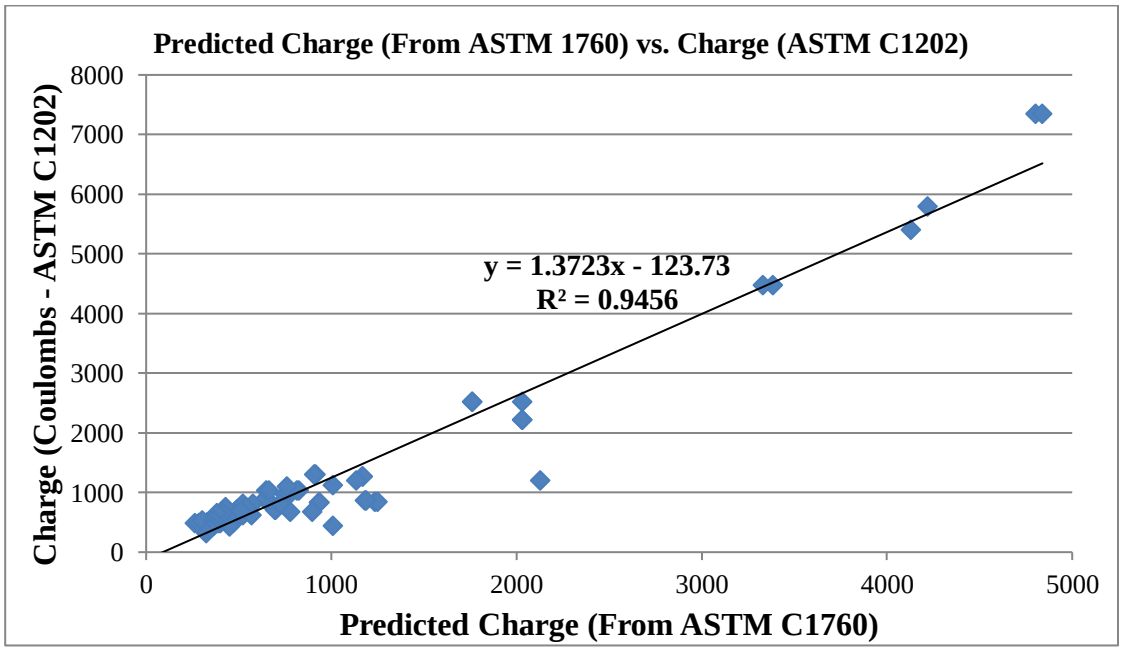

Figure 4.4: Charge (Coulombs) from ASTM C1202 vs. Predicted Charge Using Bulk Conductivity (ASTM C1760)

Figure 4.5 shows that most of the results for predicted charge, using ASTM C1760, yield lower results than those measured using ASTM C1202 (% Error > 0%). This is expected due to the "Joule Effect" present during the ASTM C1202 test, which increases the current (***I***) over the 6-hour test period. The majority of the predicted charge values are 16 to 38% lower than the charge obtained using ASTM C1202, as shown in Figure 4.5. It should be noted that the precision for an average of 3 samples as stated in ASTM C1202 is 42%, therefore the majority of these test results were within the precision of the standard (ASTM C1202, 2018).

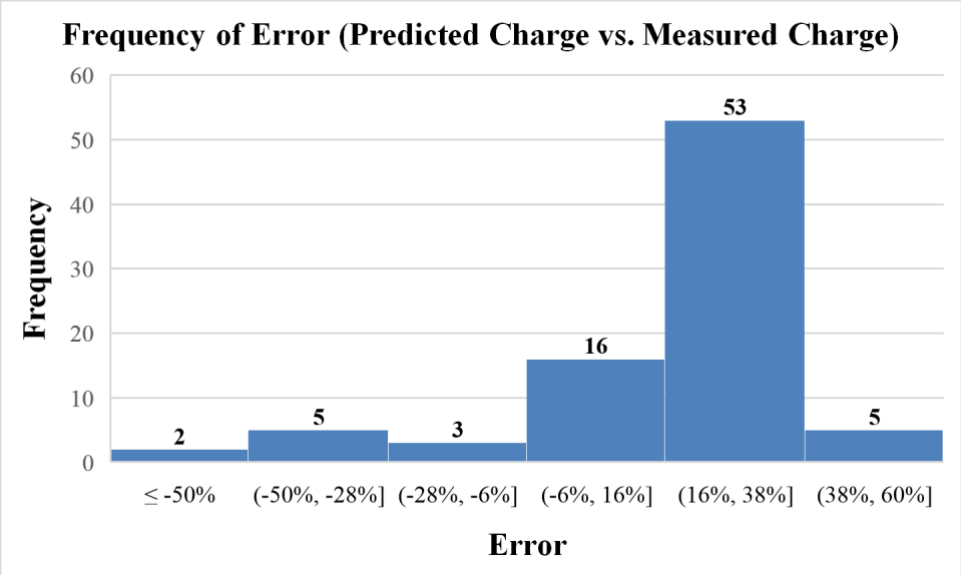

Figure 4.5: Frequency of Error, Predicted Charge (ASTM C1760) vs. Measured Charge (ASTM C1202)

4.4 In-Situ Testing of Concrete using Surface Resistivity (SR)

Surface resistivity (SR) measurements using the Resipod 4-point Wenner probe were taken from four separate concrete elements of three newly built, or rehabilitated, NBDTI bridge structures at 56 days to provide a comparison to the SR measurements

performed on lab cured cylinders. After the initial measurements were taken in the field, and the large variances observed, research was conducted to determine the variabilities present when measuring SR in-situ rather than from thoroughly saturated concrete specimens in the laboratory. It was determined that the presence and location of reinforcing steel, degree of saturation and concrete surface temperature all play an important role in obtaining accurate measurements. Due to the scope of this study and the limit of resources to thoroughly address these issues when performing measurements in the field, this portion of the research was not expanded past the data shown in Figure 4.6.

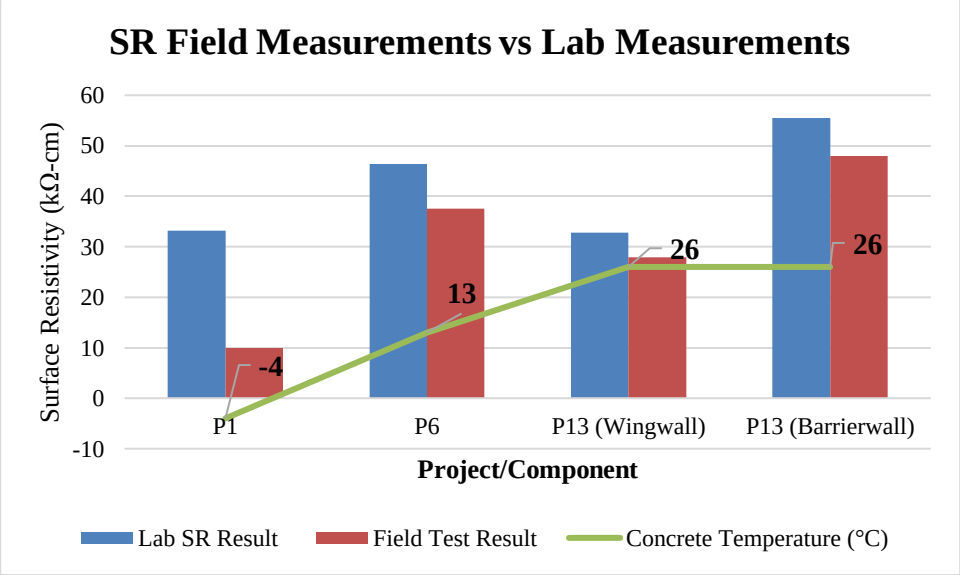

Figure 4.6: Surface Resistivity Field Measurements vs. Lab Measurements for four Concrete Components.

Figure 4.6 tends to show the opposite relationship expected when taking SR measurements at lower temperatures. It is commonly known that a lower concrete temperature will increase the electrical resistivity of a concrete material. However, the

SR field results tended to differ the most from the lab results when concrete temperatures were the lowest (P1 and P2). No additional measures were taken to saturate the surface of the concrete either, therefore the concrete itself was thought to be in a semi-saturated condition and would possibly yield higher results because of this (see Figure 2.7 in Section 2.5).

The reinforcing steel cover for all field investigations was 60-mm to 70-mm. Proceq, as well as other literature, states that electrical resistivity measurements can be affected by the presence of reinforcing steel, particularly when the cover depth is less than 30-mm (Proceq, 2017).

The final factor, and one that the author feels is an important contributing factor, is the ambient temperature at which the concrete was cured from the time it was placed until 56 days. Table 4.1 lists the average ambient temperature over the 56-day period that each concrete element was subjected to, which is dependent on the time of year it was placed. Project 1 (P1), which showed the lowest field SR measurements in relation to lab cured measurements, was cured in the coldest average ambient temperature until the time of test and very likely affected the quality of the material, thus yielding lower results. The field SR measurements taken from concrete elements cured in more favorable conditions (P3), showed results that more closely reflected the lab measurements. It is worth noting that none of the average 56-day ambient curing conditions matched the minimum 21°C required in CSA A23.2-3C for lab curing of concrete specimens.

Table 4.1: Average Ambient Temperature Over 8-week Curing Period

Project	Average Ambient Curing Temperature (From Environment Canada)
P1	3.2°C
P2	5.4°C
P3 (Wingwall)	12.7°C
P3 (Barrierwall)	17.2°C

4.5 Temperature Effect on Surface Resistivity

Concrete cylinders from lab mixes 2 and 4 were subjected to temperature treatments as described in Section 3.5 to quantify the effect temperature has on surface resistivity of concrete. As shown in Figure 4.7, as the temperature of the concrete increases, the electrical resistivity decreases.

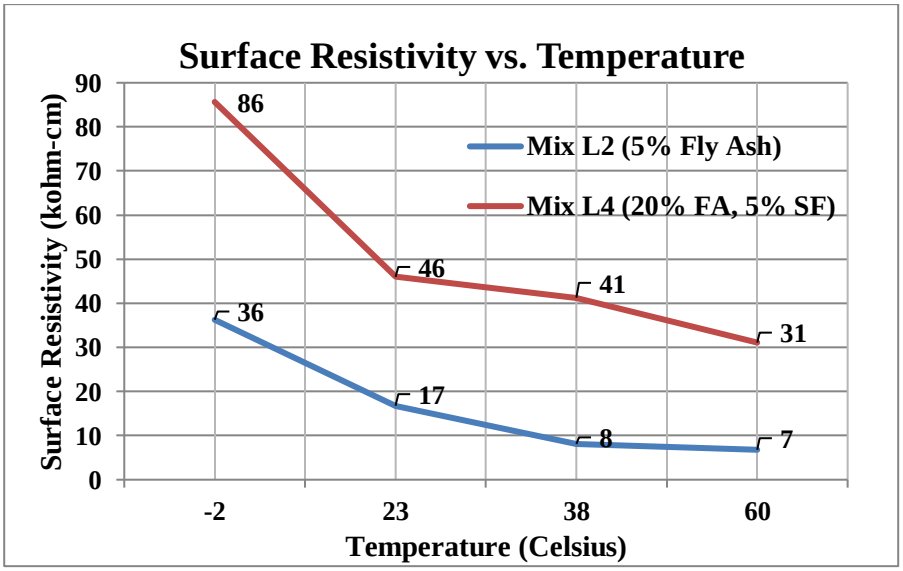

Figure 4.7: Surface Resistivity vs. Measured Temperature for Mixes L2 and L4

Liu and Presuel-Moreno (2014) reported that Arrhenius Law can be used to normalize electrical resistivity measurements taken at various temperatures to a baseline temperature. Arrhenius Law is shown as Equation 4.1,

$$\boldsymbol{\rho_t = \rho_0 \cdot exp\left[\frac{E_{a,\rho}}{R}\left(\frac{1}{T} - \frac{1}{T_0}\right)\right]} \qquad \textbf{Eq. 4.1}$$

where $\boldsymbol{\rho_t}$ is the resistivity measured at temperature $\boldsymbol{T}$, $\boldsymbol{\rho_0}$ is the resistivity at reference temperature $\boldsymbol{T_0}$, $\boldsymbol{R}$ is the gas constant (8.314 J/mol K) and $\boldsymbol{E_{a,\rho}}$ is the activation energy for concrete resistivity (J/mol).

The activation energy is different with every concrete material and depends heavily on the mix design of the concrete material, with SCM's having been reported to increase the activation energy relative to OPC mixes. Liu and Presuel-Moreno (2014) suggested Equations 4.2 and 4.3 to calculate the activation energy of concrete,

$$\boldsymbol{E_{a,\rho} = 3.7738\, ln(\rho_{23}) + 9.7518} \qquad \textbf{Eq. 4.2}$$

$$\boldsymbol{E_{a,\rho} = 6.0157\, ln(\rho_{23}) + 4.3121} \qquad \textbf{Eq. 4.3}$$

where $\boldsymbol{\rho_{23}}$ is the measured resistivity at a baseline temperature of 23°C. Equation 4.2 was proposed for concretes with >20% fly ash, and Equation 4.3 for concretes with less than 20% Fly Ash. Arrhenius Law was then used to normalize resistivity values measured at the temperatures shown in Figure 4.7 to 23°C. The results for comparison are shown in Table 4.2. As shown by the error calculation comparing the normalized resistivity and the resistivity measured at 23°C, Arrhenius Law, with the activation energy equations presented above, fits better for mix L2 than it does for mix L4. The SR

measurements made at -18°C were omitted from Figure 4.7 and Table 4.2 as they further exacerbated the poor fit of the data to Arrhenius Law. This is thought to be caused by the freezing of the concrete pore solution, which increases electrical resistivity as electrical current cannot pass through the concrete system. Appendix E presents the complete tabulated results for surface resistivity on temperature treated concrete.

Table 4.2: Electrical Resistivity Measurements Normalized to 23°C

	Mix L2 (5% Fly Ash)				Mix L4 (20% FA, 5% SF)			
Specimen Temperature (°C)	**60**	**38**	**23**	**-2**	**60**	**38**	**23**	**-2**
Avg. Surface Resistivity	**6.8**	**8.1**	**16.8**	**36.3**	**31.1**	**41.3**	**46.0**	**85.7**
Temperature (Kelvin)	333.2	311.2	296.2	271.2	333.2	311.2	296.2	271.2
Resistivity (Normalized to 23C)	**17.7**	**12.3**	**16.8**	**16.3**	**92.6**	**66.3**	**46.0**	**34.6**
Error	**6%**	**-27%**	**0%**	**-3%**	**101%**	**44%**	**0%**	**-25%**

4.6 Cost Analysis

Surface resistivity testing provides many attractive benefits to any transportation agency when compared to ASTM C1202. The typical time to test a cylinder for SR using the Resipod 4-point Wenner probe device is in the range of five minutes, which is a significant advantage over the nearly 2-day process of performing a RCP test as per ASTM C1202.

During the 2017 construction season, NBDTI had 269 concrete specimens tested for RCP by an independent laboratory as part of its quality assurance specifications,

which represents a significant cost to NBDTI. Icenogle and Rupnow (2011) completed a study at the Louisiana Transportation Research Center that compared the cost of performing SR versus RCP testing over the span of one year. The study concluded that the total annual cost of SR testing was merely 6% of the total cost of performing RCP tests as had been performed by the Louisiana Department of Transportation and Development (LADOTD) at that point in time. LADOTD have since developed a procedure and have implemented SR testing for quality assurance (Icenogle and Rupnow, 2011). Similar measures could be undertaken by any transportation agency to reduce costs and still receive quality test results by simply changing test methods.

5 CONCLUSIONS AND RECOMMENDATIONS

The purpose of this study was to determine if electrical resistivity was a suitable supplement or replacement for the commonly used RCP test (ASTM C1202) using concrete mixes commonly supplied for NBDTI projects. Measurements were performed on lab-cured cylinders to determine the correlation of surface resistivity, bulk resistivity and bulk conductivity to results obtained from RCP testing. Surface resistivity measurements were also taken in the field on four newly placed concrete elements from 3 separate structures to determine the viability of using SR testing in-situ for quality assurance. The following sections outline the conclusions and recommendations taken from this study.

5.1 Conclusions

1. Surface resistivity testing using the Resipod 4-point Wenner probe and bulk resistivity testing using the RCON device by Giatec Scientific both show a good correlation to RCP testing and could be utilized as a supplement to or replacement of RCP (ASTM C1202) for quality assurance testing for typically used NBDTI concrete materials. Both test methods provide a further benefit over RCP testing in that they are non-destructive to the concrete cylinder specimen, enabling it to be utilized for further testing. Both test methods are also quicker to perform and have been reported in the literature to be more repeatable than the RCP test.

The SR threshold limits established (equating SR tests to an RCP value of 1000 coulombs) were significantly lower than the limits stated by four other transportation agencies and research groups.

2. Bulk conductivity testing using ASTM C1760 shows a good correlation to results obtained from the RCON for bulk resistivity when resistivity is calculated from the current measured at 1 minute from the bulk conductivity test using Equation 7.

   Bulk conductivity shows a good correlation when used to predict the total charge (in coulombs) through a 50-mm length concrete sample over a period of 6 hours in comparison to results obtained for RCP testing using ASTM C1202. The predicted total charge tends to be less than the results using ASTM C1202, which could be in part due to the elimination of the sample temperature increase or "Joule Effect". Similar to SR and BR, this test method also carries the further benefit of being non-destructive to the concrete cylindrical specimen and it is quicker and simpler to perform, which could lead to potential cost savings.

3. Surface resistivity measurements in the field on concrete in-situ appear to be able to give an indication of concrete quality, however it may not be suitable as a quality assurance tool where pay adjustments are used in contract specifications without the development of precise adjustment factors for concrete temperature, degree of saturation and the presence of reinforcing steel.

4. Using Arrhenius Law to normalize resistivity measurements to a baseline temperature of 23°C appears to fit better to mix L2, containing 5% fly ash. Arrehnuis Law does not fit as well to mix L4, containing 20% fly ash and 5% silica fume. This could be in part due to the use of Equations 4.2 and 4.3 to calculate the activation energy of various types of concrete mix designs. Measurements made on concrete conditioned to -18°C appeared to further exacerbate the poor fit of Arrhenius Law, but this was likely due to the fact that the pore solution of the concrete was frozen, thus increasing the electrical resistivity of the sample as electrical current could not pass through the system.

5. The cost of implementing surface resistivity testing has been reported to be merely 6% of the cost of RCP testing for quality assurance. This provides a significant savings to any transportation agency.

5.2 Recommendations

The author recommends the following further research based on the findings of this study:

1. Further testing to establish a numerical relationship associated with various dosages of calcium nitrite corrosion inhibitor (CNI) for both surface resistivity and bulk resistivity measurements using various local concrete mix designs.
2. Further in-situ surface resistivity testing using various techniques to saturate the in-situ concrete and more methodical locating of the reinforcing steel to establish a range of correction factors for the limitations associated with in-situ resistivity testing stated in this study.

3. Further testing to correlate the results established for electrical resistivity testing with diffusion coefficients (ASTM C1556), using local New Brunswick materials to ensure that electrical methods correlate to direct permeability measurements.

6 REFERENCES

AASHTO TP 95-14. (2014). *Method of Test for Surface Resistivity Indication of Concretes Ability to Resist Chloride Ion Penetration*. Washington, DC: American Association of State Highway and Transportation Officials.

ACI 308R-16. (2016). ACI Manual of Concrete Practice. *Guide to External Curing of Concrete*. Farmington Hills, MI: American Concrete Institute.

ASTM Draft 7. (2015, June 12). *Standard Test Method for Bulk Resistivity of Concrete*. West Conshohocken, PA: ASTM International.

ASTM Standard 1543-10a. (2010). *Standard Test Method for Determining the Penetration of Chloride Ion into Concrete by Ponding.* Retrieved from ASTM International, West Conshohocken, PA: www.astm.org

ASTM Standard C1202-18. (2009). *Standard Test Method for Electrical Indication of Concrete's Ability to Resist Chloride Ion Penetration.* Retrieved from ASTM International, West Conshohocken, PA: www.astm.org

ASTM Standard C1556-11a. (2011). *Standard Test Method for Determining the Apparent Chloride Diffusion Coefficient of Cementitious Mixtures by Bulk Diffusion.* Retrieved from ASTM International, West Conshohocken, PA: www.astm.org

ASTM Standard C1760-12. (2012). *Standard Test Method for Bulk Electrical Conductivity of Hardened Concrete.* Retrieved from ASTM International, West Conshohocken, PA: www.astm.org

CAN/CSA-S6-06. (2006). *Canadian Highway Bridge Design Code.* Mississauga, ON: CSA Group.

CSA A23.1-14/A23.2-14. (2014). *Concrete materials and methods of concrete construction/Test Methods and standard practices for concrete.* Mississauga, ON: CSA Group.

Elkey, W., & Sellevold, E. (1995). Electrical Resistivity of Concrete. *Norwegian Public Roads Administration Publication*, 33.pp.

Germann Instruments. (2018, November 11). *Complete Proove'it Brochure.* Retrieved from Germann Instruments Website: http://germann.org/wp-content/uploads/2016/06/Proove_it.pdf

Ghosh, P., & Tran, Q. (2015). Correlation Between Bulk and Surface Resistivity of Concrete. *International Journal of Concrete Structures and Materials*, Vol. 9, No. 1, pp. 119-132.

Giatec Scientific. (2018, November 11). *RCON User Manual.* Retrieved from Giatec Scientific: https://www.giatecscientific.com/wp-content/uploads/2013/06/Giatec-RCON-DS-v14-01.pdf

Giatec Scientific. (2018, November 11). *RCON2 User Manual.* Retrieved from Giatec Scientific: Giatec Scientific.

Hamilton III, H., Boyd, A., Vivas, E., & Bergin, M. (2007). *Permeability of Concrete - Comparison of Conductivity and Diffusion Methods.* Gainesville: University of Florida - Department of Civil & Coastal Engineering.

Icenogle, T., & Rupnow, P. (2011). *Evaluation of Surface Resistivity Measurements as an Alternative to the Rapid Chloride Permeability Test for Quality Assurance and Acceptance.* Baton Rouge: Lousiana Transportation Research Center.

Isgor, M., & Morales, B. (2015). *Improved Corrosion Inspection Procedures for Reinforced Concrete Bridges: Electrical Resistivity of Concrete.* Seattle: PacTrans & Oregon State University.

Liu, Y., & Presuel-Moreno. (2014). Normalization of Temperature Effect on Concrete Resistivity by Method of Arrhenius Law. *ACI Materials Journal, July-August* , 433-442.

Liu, Y., Presuel-Moreno, F., & Paredes, M. (2015). Determination of Chloride Diffusion Coefficients in Concrete by Electrical Resistivity Method. *ACI Materials Journal, September-October*, 631-640.

Marquez, J. (2015). *Influence of Saturation and Geometry on Surface Electrical Resistivity Measurements.* Montreal: Concordia University.

Morris, W., Moreno, E., & Sagues, A. (1996). *Practical Evaluation of Resistivity of Concrete in Test Cylinders Using a Wenner Array Probe.* Tampa: University of Florida, Department of Civil and Environmental Engineering.

Nassif, H., Rabie, S., Na, C., & Salvador, M. (2015). *Evaluation of Surface Resistivity Indication of Ability of Concrete to Resist Chloride Ion Penetration.* Piscataway, NJ.: Rutgers Infrastructure Monitoring and Evaluation (RIME) Group.

NBDTI. (2015). *2015 NBDTI Standard Specifcations*. Fredericton, NB: New Brunswick Department of Transportation & Infrastructure.

Neville, A. (2011). *Properties of Concrete, 5th Edition.* Essex: Prentice Hall.

Proceq. (2017). *Proceq Resipod Brochure.* Retrieved from Proceq: https://www.proceq.com/uploads/tx_proceqproductcms/import_data/files/Resipod_Sales%20Flyer_English_high.pdf

Riding, K., Poole, J., Schindler, A., Juenger, M., & Folliard, K. (2008). Simplified Concrete Resistivity and Rapid Chloride Permeability Test Method. *ACI Materials Journal, July-August*, 390-394.

Shi, C., Stegemann, J., & Caldwell, R. (1998). Effect of Supplementary Cementing Materials on the Specific Conductivity of Pore Solution and its Implications on the Rapid Chloride Permeability Test (AASHTO T227 & ASTM C1202) Results. *ACI Materials Journal - July/August*, 389-393.

Spragg, R., Castro, J., Nantung, T., Paredes, M., & Weiss, W. (2011). *Variability Analysis of the Bulk Resistivity Measured using Concrete Cylinders.* West Lafayette: Joint Transportation Research Program - Indiana Department of Transportation and Purdue University.

Spragg, R., Villani, C., Snyder, K., Bentz, D., Bullard, J., & Weiss, J. (2012). Electrical Resistivity Measurements in Cementitious Systems: Observations of Factors that Influence the Measurements. *92nd Annual Transportation of the Transportation Research Board.* Washington: Transportation Research Board - 2013 Annual Meeting.

Stanish, K., Hooton, R., & Thomas, M. (1997). *Testing the Chloride Penetration Resistance of Concrete: A Literature Review.* Toronto: University of Toronto, Department of Civil Engineering.

Thomas, M. (2013). *Supplementary Cementing Materials in Concrete.* Boca Raton: CRC Press.

Thomas, M. (2014). CE 6503 Course Notes. Fredericton, NB: University of New Brunswick - Department of Civil Engineering.

Thomas, M. (2014). CE 6563 Course Notes. Fredericton, NB: University of New Brunswick - Department of Civil Engineering.

Van Nostrand, R. G., & Cook, K. (1966). *Interpretation of Resistivity Data* . Washington: United States Government Printing Office.

Whiting, D., & Mitchell, T. (1992). History of the Rapid Chloride Permeability Test. *Transportation Research Record 1335*, 55-62.

APPENDIX A – Surface Resistivity Tabulated Results

Project ID	Placement #	Sample ID	Date Cast	Date Tested	Length (mm)	Diameter (mm)	4 Point Probe (kΩ-cm)	4 Point Probe (Adjusted) (kΩ-cm)
P2	19	35L	4-Sep	30-Oct	200.7	101.5	**56.3**	**28.9**
P2	19	35K	4-Sep	30-Oct	199.5	101.5	**54.5**	**27.9**
P2	22	38J	17-Sep	12-Nov	196.4	101.5	**68.7**	**35.2**
P2	22	38K	17-Sep	12-Nov	196.3	101.5	**69.4**	**35.6**
P2	23	39J	6-Oct	1-Dec	198.0	101.5	**74.0**	**37.9**
P2	23	39K	6-Oct	1-Dec	199.9	101.5	**73.3**	**37.6**
P2	24	42J	9-Oct	4-Dec	200.2	101.5	**64.7**	**33.2**
P2	24	42K	9-Oct	4-Dec	196.7	101.5	**70.1**	**35.9**
P10	13	37A	19-Aug	14-Oct	198.7	101.5	**100.9**	**51.7**
P10	13	37B	19-Aug	14-Oct	198.6	101.5	**100.8**	**51.7**
P10	21	50E	17-Sep	13-Nov	202.0	101.5	**77.1**	**39.5**
P10	21	50D	17-Sep	13-Nov	201.8	101.5	**79.8**	**40.9**
P10	24	54D	1-Oct	26-Nov	203.4	101.5	**71.7**	**36.8**
P10	24	54E	1-Oct	26-Nov	202.7	101.5	**70.9**	**36.4**
P10	26	57	9-Oct	4-Dec	199.7	101.5	**68.9**	**35.3**
P10	26	57	9-Oct	4-Dec	201.9	101.5	**69.9**	**35.8**
P7	3	11Q	13-Aug	8-Oct	200.5	101.5	**72.2**	**37.0**
P7	3	11R	13-Aug	8-Oct	200.5	101.5	**69.2**	**35.5**
P6	10	18K	13-Aug	8-Oct	201.0	101.5	**39.7**	**20.4**
P6	10	18L	13-Aug	8-Oct	201.0	101.5	**39.0**	**20.0**
P6	11	22K	17-Aug	12-Oct	200.5	101.5	**40.6**	**20.8**
P6	11	22L	17-Aug	12-Oct	200.3	101.5	**39.3**	**20.2**
P6	12	25K	18-Aug	13-Oct	199.3	101.5	**36.7**	**18.8**
P6	12	25L	18-Aug	13-Oct	199.0	101.5	**37.0**	**19.0**
P6	13	26K	2-Sep	28-Oct	199.2	101.5	**31.4**	**16.1**
P6	13	26L	2-Sep	28-Oct	198.6	101.5	**31.8**	**16.3**
P6	14	28L	3-Sep	29-Oct	201.7	101.5	**43.0**	**22.1**
P6	14	28K	3-Sep	29-Oct	199.0	101.5	**43.8**	**22.5**
P1	1	1K	20-Aug	15-Oct	200.8	101.5	**36.3**	**18.6**
P1	1	1L	20-Aug	15-Oct	201.1	101.5	**34.8**	**17.8**
P1	2	2L	26-Aug	21-Oct	198.4	101.5	**49.1**	**25.2**
P1	2	2K	26-Aug	21-Oct	197.6	101.5	**49.4**	**25.3**
P1	3	3L	28-Aug	23-Oct	197.4	101.5	**50.0**	**25.6**
P1	3	3K	28-Aug	23-Oct	198.6	101.5	**54.5**	**27.9**
P1	4	4L	31-Aug	26-Oct	199.3	101.5	**53.9**	**27.6**
P1	4	4K	31-Aug	26-Oct	198.7	101.5	**53.9**	**27.6**

P1	5	5L	2-Sep	28-Oct	201.0	101.5	**64.9**	**33.3**
P1	5	5K	2-Sep	28-Oct	201.0	101.5	**64.9**	**33.3**
P1	6	6L	4-Sep	30-Oct	198.8	101.5	**78.1**	**40.1**
P1	6	6K	4-Sep	30-Oct	198.6	101.5	**74.9**	**38.4**
P1	7	7J	16-Sep	12-Nov	196.7	101.5	**33.4**	**17.1**
P1	7	7K	16-Sep	12-Nov	200.1	101.5	**34.9**	**17.9**
P1	8	8J	24-Sep	19-Nov	197.1	101.5	**45.2**	**23.2**
P1	8	8K	24-Sep	19-Nov	202.9	101.5	**51.4**	**26.4**
P1	9	9J	25-Sep	19-Nov	196.7	101.5	**33.1**	**17.0**
P1	9	9K	25-Sep	19-Nov	200.5	101.5	**32.8**	**16.8**
P1	10	10J	2-Oct	27-Nov	196.9	101.5	**90.7**	**46.5**
P1	10	10K	2-Oct	27-Nov	201.6	101.5	**90.3**	**46.3**
P1	11	11J	8-Oct	3-Dec	196.6	101.5	**90.5**	**46.4**
P1	11	11K	8-Oct	3-Dec	195.8	101.5	**90.4**	**46.4**
P1	12	12J	15-Oct	10-Dec	199.2	101.5	**83.4**	**42.8**
P1	12	12K	15-Oct	10-Dec	200.5	101.5	**87.9**	**45.1**
P4	2	3P	28-Sep	23-Nov	201.4	101.5	**115.4**	**59.2**
P4	2	3Q	28-Sep	23-Nov	200.4	101.5	**113.4**	**58.2**
P4	3	6N	5-Oct	30-Nov	193.7	101.5	**111.5**	**57.2**
P4	3	6O	5-Oct	30-Nov	194.7	101.5	**113.6**	**58.3**
P4	4	8N	7-Oct	2-Dec	197.1	101.5	**119.7**	**61.4**
P4	4	8O	7-Oct	2-Dec	196.1	101.5	**114.5**	**58.7**
P4	5	9N	12-Oct	7-Dec	193.6	101.5	**90.3**	**46.3**
P4	5	9O	12-Oct	7-Dec	194.4	101.5	**90.0**	**46.2**
P4	6	12N	14-Oct	9-Dec	195.5	101.5	**111.7**	**57.3**
P4	6	12O	14-Oct	9-Dec	189.1	101.5	**112.9**	**57.9**
P4	7	14N	15-Oct	10-Dec	197.0	101.5	**82.8**	**42.5**
P4	7	14O	15-Oct	10-Dec	194.6	101.5	**88.9**	**45.6**
P2	3	5H	10-Oct	5-Dec	196.7	101.5	**63.6**	**32.6**
P2	3	7H	10-Oct	5-Dec	193.7	101.5	**79.3**	**40.7**
P5	26	47J	21-Oct	15-Dec	195.0	101.5	**83.2**	**42.7**
P5	26	47K	21-Oct	15-Dec	197.4	101.5	**81.8**	**41.9**
P4	8	17O	21-Oct	16-Dec	195.5	101.5	**106.3**	**54.5**
P4	8	18L	21-Oct	16-Dec	195.5	101.5	**94.7**	**48.6**
P3	5	12D	16-Oct	11-Dec	199.3	101.5	**86.1**	**44.2**
P3	9	18X	12-Nov	7-Jan	197.6	101.5	**98.5**	**50.5**
P3	9	18Y	12-Nov	7-Jan	200.8	101.5	**108.9**	**55.8**
P3	10	20Y	13-Nov	8-Jan	200.5	101.5	**118.2**	**60.6**
P8	6	6Q	10-Nov	12-Jan	188.8	101.5	**65.3**	**33.5**
P11	1	1H	13-Nov	7-Sep	201.0	101.5	**8.9**	**4.6**

P11	1	1I	10-Nov	7-Sep	201.0	101.5	**8.5**	**4.4**
P12	1	1	27-Oct	5-Jan	200.0	101.5	**43.5**	**22.3**
P12	1	2	27-Oct	6-Jan	200.0	101.5	**47.4**	**24.3**
P12	1	3	27-Oct	6-Jan	200	101.5	**42.6**	**21.8**
L1	Lab		22-Feb-18	19-Apr-18	197.0	101.5	**7.5**	**3.8**
L1	Lab		22-Feb-18	19-Apr-18	197.0	101.5	**8.3**	**4.3**
L2	Lab		22-Feb-18	19-Apr-18	198.5	101.5	**10.9**	**5.6**
L2	Lab		22-Feb-18	19-Apr-18	198.0	101.5	**10.1**	**5.2**
L3	Lab		30-Apr-18	25-Jun-18	190.0	101.5	**18.2**	**9.3**
L3	Lab		30-Apr-18	25-Jun-18	190.0	101.5	**21.4**	**11.0**
L4	Lab		30-Apr-18	25-Jun-18	197.0	101.5	**16.6**	**8.5**
L4	Lab		30-Apr-18	25-Jun-18	197.0	101.5	**16.8**	**8.6**
L4	Lab		30-Apr-18	25-Jun-18	197.0	101.5	**16.8**	**8.6**
L6	Lab		30-Apr-18	25-Jun-18	199.0	101.5	**109.3**	**56.1**
L5	Lab		30-Apr-18	25-Jun-18	198.5	101.5	**46.0**	**23.6**
P13	33	66I	3-May-18	28-Jun-18	200.0	101.5	**64.0**	**32.8**
P13	36	72I	30-May-18	25-Jul-18	200	101.5	**108.3**	**55.5**

APPENDIX B – Bulk Resistivity Tabulated Results

Project ID	Placement #	Sample ID	Date Cast	Date Tested	Length, (mm)	Diameter, (mm)	Z (Ω)	RCON (kΩ-cm)
P2	19	35L	4-Sep	30-Oct	200.7	101.5	6.98	**28.1**
P2	19	35K	4-Sep	30-Oct	199.5	101.5	6.94	**28.1**
P2	22	38J	17-Sep	12-Nov	196.4	101.5	8.75	**36.0**
P2	22	38K	17-Sep	12-Nov	196.3	101.5	8.42	**34.7**
P2	23	39J	6-Oct	1-Dec	198.0	101.5	9.25	**37.8**
P2	23	39K	6-Oct	1-Dec	199.9	101.5	9.15	**37.0**
P2	24	42J	9-Oct	4-Dec	200.2	101.5	8.18	**33.0**
P2	24	42K	9-Oct	4-Dec	196.7	101.5	8.30	**34.1**
P10	13	37A	19-Aug	14-Oct	198.7	101.5	12.7	**51.7**
P10	13	37B	19-Aug	14-Oct	198.6	101.5	13.3	**54.2**
P10	21	50E	17-Sep	13-Nov	202.0	101.5	10.0	**39.9**
P10	21	50D	17-Sep	13-Nov	201.8	101.5	10.7	**42.9**
P10	24	54D	1-Oct	26-Nov	203.4	101.5	9.6	**38.2**
P10	24	54E	1-Oct	26-Nov	202.7	101.5	9.6	**38.4**
P10	26	57	9-Oct	4-Dec	199.7	101.5	9.2	**37.1**
P10	26	57	9-Oct	4-Dec	201.9	101.5	9.1	**36.6**
P7	3	11Q	13-Aug	8-Oct	200.5	101.5	9.3	**37.7**
P7	3	11R	13-Aug	8-Oct	200.5	101.5	9.4	**37.8**
P6	10	18K	13-Aug	8-Oct	201.0	101.5	5.15	**20.7**
P6	10	18L	13-Aug	8-Oct	201.0	101.5	5.13	**20.6**
P6	11	22K	17-Aug	12-Oct	200.5	101.5	5.45	**22.0**
P6	11	22L	17-Aug	12-Oct	200.3	101.5	4.93	**19.9**
P6	12	25K	18-Aug	13-Oct	199.3	101.5	4.62	**18.7**
P6	12	25L	18-Aug	13-Oct	199.0	101.5	4.72	**19.2**
P6	13	26K	2-Sep	28-Oct	199.2	101.5	4.26	**17.3**
P6	13	26L	2-Sep	28-Oct	198.6	101.5	4.05	**16.5**
P6	14	28L	3-Sep	29-Oct	201.7	101.5	6.14	**24.6**
P6	14	28K	3-Sep	29-Oct	199.0	101.5	5.94	**24.1**
P1	1	1K	20-Aug	15-Oct	200.8	101.5	4.63	**18.6**
P1	1	1L	20-Aug	15-Oct	201.1	101.5	4.65	**18.7**
P1	2	2L	26-Aug	21-Oct	198.4	101.5	6.31	**25.7**
P1	2	2K	26-Aug	21-Oct	197.6	101.5	6.47	**26.5**
P1	3	3L	28-Aug	23-Oct	197.4	101.5	6.50	**26.6**
P1	3	3K	28-Aug	23-Oct	198.6	101.5	6.58	**26.8**
P1	4	4L	31-Aug	26-Oct	199.3	101.5	6.80	**27.6**
P1	4	4K	31-Aug	26-Oct	198.7	101.5	6.65	**27.1**

P1	5	5L	2-Sep	28-Oct	201.0	101.5	8.10	**32.6**
P1	5	5K	2-Sep	28-Oct	201.0	101.5	8.34	**33.6**
P1	6	6L	4-Sep	30-Oct	198.8	101.5	9.03	**36.7**
P1	6	6K	4-Sep	30-Oct	198.6	101.5	8.99	**36.6**
P1	7	7J	16-Sep	12-Nov	196.7	101.5	4.44	**18.3**
P1	7	7K	16-Sep	12-Nov	200.1	101.5	4.52	**18.3**
P1	8	8J	24-Sep	19-Nov	197.1	101.5	5.56	**22.8**
P1	8	8K	24-Sep	19-Nov	202.9	101.5	6.3	**25.0**
P1	9	9J	25-Sep	19-Nov	196.7	101.5	4.3	**17.8**
P1	9	9K	25-Sep	19-Nov	200.5	101.5	4.3	**17.2**
P1	10	10J	2-Oct	27-Nov	196.9	101.5	10.8	**44.4**
P1	10	10K	2-Oct	27-Nov	201.6	101.5	11.2	**44.9**
P1	11	11J	8-Oct	3-Dec	196.6	101.5	10.5	**43.2**
P1	11	11K	8-Oct	3-Dec	195.8	101.5	10.1	**41.7**
P1	12	12J	15-Oct	10-Dec	199.2	101.5	11.6	**47.1**
P1	12	12K	15-Oct	10-Dec	200.5	101.5	11.1	**44.8**
P4	2	3P	28-Sep	23-Nov	201.4	101.5	14.3	**57.4**
P4	2	3Q	28-Sep	23-Nov	200.4	101.5	13.9	**56.1**
P4	3	6N	5-Oct	30-Nov	193.7	101.5	13.6	**56.8**
P4	3	6O	5-Oct	30-Nov	194.7	101.5	13.3	**55.2**
P4	4	8N	7-Oct	2-Dec	197.1	101.5	14.2	**58.3**
P4	4	8O	7-Oct	2-Dec	196.1	101.5	14.2	**58.6**
P4	5	9N	12-Oct	7-Dec	193.6	101.5	11.1	**46.4**
P4	5	9O	12-Oct	7-Dec	194.4	101.5	10.7	**44.5**
P4	6	12N	14-Oct	9-Dec	195.5	101.5	13.4	**55.4**
P4	6	12O	14-Oct	9-Dec	189.1	101.5	13.6	**58.2**
P4	7	14N	15-Oct	10-Dec	197.0	101.5	10.3	**42.3**
P4	7	14O	15-Oct	10-Dec	194.6	101.5	10.7	**44.5**
P2	3	5H	10-Oct	5-Dec	196.7	101.5	8.7	35.6
P2	3	7H	10-Oct	5-Dec	193.7	101.5	9.7	40.5
P5	26	47J	21-Oct	15-Dec	195.0	101.5	9.62	**39.9**
P5	26	47K	21-Oct	15-Dec	197.4	101.5	9.42	**38.6**
P4	8	17O	21-Oct	16-Dec	195.5	101.5	11.8	**48.8**
P4	8	18L	21-Oct	16-Dec	195.5	101.5	11.5	**47.6**
P3	5	12D	16-Oct	11-Dec	199.3	101.5	11.0	**44.6**
P3	9	18X	12-Nov	7-Jan	197.6	101.5	13.5	**55.3**
P3	9	18Y	12-Nov	7-Jan	200.8	101.5	14.2	**57.2**
P3	10	20Y	13-Nov	8-Jan	200.5	101.5	15.4	**62.1**
P8	6	6Q	10-Nov	12-Jan	188.8	101.5	8.2	**35.3**
P11	1	1H	13-Nov	7-Sep	201.0	101.5	1.2	**4.9**

P11	1	1I	10-Nov	7-Sep	201.0	101.5	1.3	**5.0**
P12	1	1	27-Oct	5-Jan	200.0	101.5	6.1	**24.5**
P12	1	2	27-Oct	6-Jan	200.0	101.5	5.9	**24.0**
P12	1	3	27-Oct	6-Jan	200	101.5	5.9	**24.0**
L1	Lab		22-Feb-18	19-Apr-18	197.0	101.5	1.2	**5.0**
L1	Lab		22-Feb-18	19-Apr-18	197.0	101.5	1.1	**4.3**
L2	Lab		22-Feb-18	19-Apr-18	198.5	101.5	1.6	**6.5**
L2	Lab		22-Feb-18	19-Apr-18	198.0	101.5	1.5	**6.0**
L3	Lab		30-Apr-18	25-Jun-18	190.0	101.5	2.5	**10.8**
L3	Lab		30-Apr-18	25-Jun-18	190.0	101.5	2.5	**10.8**
L4	Lab		30-Apr-18	25-Jun-18	197.0	101.5	2.3	**9.3**
L4	Lab		30-Apr-18	25-Jun-18	197.0	101.5	2.3	**9.3**
L4	Lab		30-Apr-18	25-Jun-18	197.0	101.5	2.3	**9.3**
L6	Lab		30-Apr-18	25-Jun-18	199.0	101.5	13.8	**56.1**
L5	Lab		30-Apr-18	25-Jun-18	198.5	101.5	6.1	**24.7**
P13	33	66I	3-May-18	28-Jun-18	200.0	101.5		
P13	36	72I	30-May-18	25-Jul-18	200	101.5		

APPENDIX C – Bulk Conductivity Tabulated Results

Project ID	Sample ID	Length (mm)	Dia. (mm)	Current (mA)	Voltage (V)	σ (mS/m)	Pred. Charge (Coulombs)	Adj Pred. Charge (Coulombs)	Resistivity (kΩ-cm)
P2	35L	200.7	101.5	8.4	60.0	**3.47**	**741.8**	**653.2**	**28.8**
P2	35K	199.5	101.5	8.3	60.0	**3.41**	**728.6**	**641.6**	**29.3**
P2	38J	196.4	101.5	6.5	60.0	**2.63**	**561.7**	**494.7**	**38.0**
P2	38K	196.3	101.5	6.4	60.0	**2.59**	**552.8**	**486.8**	**38.6**
P2	39J	198.0	101.5	6.6	60.0	**2.69**	**575.0**	**506.4**	**37.2**
P2	39K	199.9	101.5	6.4	60.0	**2.64**	**562.9**	**495.7**	**37.9**
P2	42J	200.2	101.5	6.3	60.0	**2.60**	**555.0**	**488.7**	**38.5**
P2	42K	196.7	101.5	6.6	60.0	**2.67**	**571.2**	**503.0**	**37.4**
P10	37A	198.7	101.5	3.8	60.0	**1.56**	**332.2**	**292.6**	**64.3**
P10	37B	198.6	101.5	13.1	59.9	**5.37**	**1144.7**	**1008.1**	**18.6**
P10	50E	202.0	101.5	4.9	60.0	**2.04**	**435.5**	**383.5**	**49.0**
P10	50D	201.8	101.5	4.7	60.0	**1.95**	**417.3**	**367.5**	**51.2**
P10	54D	203.4	101.5	5.9	60.0	**2.47**	**528.0**	**465.0**	**40.5**
P10	54E	202.7	101.5	6.0	60.0	**2.51**	**535.1**	**471.3**	**39.9**
P10	57	199.7	101.5	6.2	60.0	**2.55**	**544.8**	**479.8**	**39.21**
P10	57	201.9	101.5	5.9	60.0	**2.45**	**524.1**	**461.6**	**40.76**
P7	11Q	200.5	101.5						
P7	11R	200.5	101.5						
P6	18K	201.0	101.5						
P6	18L	201.0	101.5						
P6	22K	200.5	101.5	15.9	60.0	**6.57**	**1402.7**	**1235.3**	**15.2**
P6	22L	200.3	101.5	16.1	60.0	**6.64**	**1418.9**	**1249.6**	**15.1**
P6	25K	199.3	101.5	15.3	60.0	**6.28**	**1341.7**	**1181.5**	**15.9**
P6	25L	199.0	101.5	15.4	60.0	**6.31**	**1348.4**	**1187.5**	**15.8**
P6	26K	199.2	101.5	15.1	60.0	**6.20**	**1323.5**	**1165.5**	**16.1**
P6	26L	198.6	101.5	15.2	60.0	**6.22**	**1328.2**	**1169.7**	**16.1**
P6	28L	201.7	101.5	9.9	60.0	**4.11**	**878.6**	**773.7**	**24.3**
P6	28K	199.0	101.5	9.7	60.0	**3.98**	**849.3**	**748.0**	**25.2**
P1	1K	200.8	101.5	12.0	60.0	**4.96**	**1060.2**	**933.7**	**20.1**
P1	1L	201.1	101.5	12.0	60.0	**4.97**	**1061.8**	**935.1**	**20.1**
P1	2L	198.4	101.5	9.1	60.0	**3.72**	**794.4**	**699.6**	**26.9**
P1	2K	197.6	101.5	9.1	60.0	**3.70**	**791.2**	**696.8**	**27.0**
P1	3L	197.4	101.5	10.8	60.0	**4.39**	**938.0**	**826.1**	**22.8**
P1	3K	198.6	101.5	10.6	60.0	**4.34**	**926.3**	**815.7**	**23.1**
P1	4L	199.3	101.5	8.4	60.0	**3.45**	**736.6**	**648.7**	**29.0**
P1	4K	198.7	101.5	8.6	60.0	**3.52**	**751.9**	**662.1**	**28.4**

P1	5L	201.0	101.5	7.4	60.0	**3.06**	**654.5**	**576.3**	**32.6**
P1	5K	201.0	101.5	6.7	59.9	**2.78**	**592.5**	**521.8**	**36.0**
P1	6L	198.8	101.5	6.8	60.0	**2.78**	**594.8**	**523.8**	**35.9**
P1	6K	198.6	101.5	7.4	60.0	**3.03**	**646.6**	**569.5**	**33.0**
P1	7J	196.7	101.5	12.0	60.0	**4.86**	**1038.6**	**914.6**	**20.6**
P1	7K	200.1	101.5	11.7	60.0	**4.82**	**1030.1**	**907.2**	**20.7**
P1	8J	197.1	101.5	10.2	60.0	**4.14**	**884.6**	**779.0**	**24.1**
P1	8K	202.9	101.5	11.4	60.0	**4.76**	**1017.7**	**896.3**	**21.0**
P1	9J	196.7	101.5	27.9	60.0	**11.30**	**2414.7**	**2126.5**	**8.8**
P1	9K	200.5	101.5	14.6	60.0	**6.03**	**1288.0**	**1134.3**	**16.6**
P1	10J	196.9	101.5	5.0	60.0	**2.03**	**433.2**	**381.5**	**49.3**
P1	10K	201.6	101.5	5.2	60.0	**2.16**	**461.3**	**406.2**	**46.3**
P1	11J	196.6	101.5	5.1	60.0	**2.07**	**441.2**	**388.5**	**48.4**
P1	11K	195.8	101.5	5.3	60.0	**2.14**	**456.6**	**402.1**	**46.8**
P1	12J	199.2	101.5	4.7	60.0	**1.93**	**411.9**	**362.8**	**51.9**
P1	12K	200.5	101.5	4.5	60.0	**1.86**	**397.0**	**349.6**	**53.8**
P4	3P	201.4	101.5	4.2	60.0	**1.74**	**372.2**	**327.8**	**57.4**
P4	3Q	200.4	101.5	4.1	60.0	**1.69**	**361.5**	**318.4**	**59.1**
P4	6N	193.7	101.5	4.1	60.0	**1.64**	**349.4**	**307.7**	**61.1**
P4	6O	194.7	101.5	4.3	60.0	**1.72**	**368.4**	**324.4**	**58.0**
P4	8N	197.1	101.5					**0.0**	
P4	8O	196.1	101.5	4.3	60.0	**1.74**	**371.0**	**326.7**	**57.6**
P4	9N	193.6	101.5	5.0	59.9	**2.00**	**425.9**	**375.1**	**50.07**
P4	9O	194.4	101.5	5.1	60.0	**2.04**	**436.2**	**384.2**	**48.97**
P4	12N	195.5	101.5	3.5	60.0	**1.41**	**301.1**	**265.1**	**70.95**
P4	12O	189.1	101.5	3.9	59.9	**1.52**	**324.5**	**285.8**	**65.72**
P4	14N	197.0	101.5	5.8	60.0	**2.35**	**502.7**	**442.7**	**42.49**
P4	14O	194.6	101.5	5.3	60.0	**2.12**	**453.8**	**399.6**	**47.07**
P2	5H	196.7	101.5	7.1	60.0	**2.88**	**614.5**	**541.1**	**34.8**
P2	7H	193.7	101.5	5.7	60.0	**2.27**	**485.8**	**427.8**	**44.0**
P5	47J	195.0	101.5	5.5	59.9	**2.21**	**471.9**	**415.6**	**45.2**
P5	47K	197.4	101.5	5.0	60.0	**2.03**	**434.3**	**382.4**	**49.2**
P4	17O	195.5	101.5					**0.0**	
P4	18L	195.5	101.5	4.0	60.0	**1.61**	**344.1**	**303.0**	**62.08**
P3	12D	199.3	101.5	4.7	59.9	**1.93**	**412.2**	**363.0**	**51.7**
P3	18X	197.6	101.5	5.9	60.0	**2.40**	**513.0**	**451.7**	**41.6**
P3	18Y	200.8	101.5	4.6	60.0	**1.90**	**406.4**	**357.9**	**52.6**
P3	20Y	200.5	101.5	4.4	60.0	**1.82**	**388.2**	**341.8**	**55.0**
P8	6Q	188.8	101.5	7.0	60.0	**2.72**	**581.5**	**512.1**	**36.7**
P11	1H	201.0	101.5	54.2	60.0	**22.44**	**4793.4**	**4221.3**	**4.5**

P11	1I	201.0	101.5	53.0	60.0	**21.94**	**4687.3**	**4127.8**	**4.6**
P12	1	200.0	101.5	9.8	60	**4.04**	**862.4**	**759.5**	**24.8**
P12	2	200.0	101.5	13	60	**5.36**	**1144.0**	**1007.5**	**18.7**
P12	3	200	101.5						
L1		197.0	101.5	62.9	60	**25.52**	**5452.2**	**4801.4**	**3.9**
L1		197.0	101.5	63.4	60	**25.73**	**5495.5**	**4839.6**	**3.9**
L2		198.5	101.5	44	60	**17.99**	**3843.0**	**3384.3**	**5.6**
L2		198.0	101.5	43.4	60	**17.70**	**3781.0**	**3329.7**	**5.6**
L3		190.0	101.5	23.9	60	**9.35**	**1998.0**	**1759.6**	**10.7**
L3		190.0	101.5	23.9	60	**9.35**	**1998.0**	**1759.6**	**10.7**
L4		197.0	101.5	26.6	60	**10.79**	**2305.7**	**2030.5**	**9.3**
L4		197.0	101.5	26.6	60	**10.79**	**2305.7**	**2030.5**	**9.3**
L4		197.0	101.5	26.6	60	**10.79**	**2305.7**	**2030.5**	**9.3**
L6		199.0	101.5	4.2	60	**1.72**	**367.8**	**323.9**	**58.1**
L5		198.5	101.5	9.4	60	**3.84**	**821.0**	**723.0**	**26.0**
P13	66I	200.0	101.5						
P13	72I	200	101.5						

APPENDIX D – Rapid Chloride Ion Penetrability Test Results

Project ID	Placement #	Date Cast	Date Tested	Sample ID	RCP (Coulombs)	Average (Coulombs)
P2	19	4-Sep	30-Oct	35G	820.9	**882.0**
P2	19	4-Sep	30-Oct	35H	943.1	
P2	22	17-Sep	12-Nov	38G	670.3	**654.7**
P2	22	17-Sep	12-Nov	38H	639.0	
P2	23	6-Oct	1-Dec	39G	725.5	**719.1**
P2	23	6-Oct	1-Dec	39H	712.7	
P2	24	9-Oct	4-Dec	42G	723.8	**704.7**
P2	24	9-Oct	4-Dec	42H	685.5	
P10	13	19-Aug	14-Oct	37O	431.5	**440.5**
P10	13	19-Aug	14-Oct	37P	449.4	
P10	21	17-Sep	13-Nov	50O	503.5	**480.7**
P10	21	17-Sep	13-Nov	50P	457.9	
P10	24	1-Oct	26-Nov	54O	511.1	**499.7**
P10	24	1-Oct	26-Nov	54P	488.3	
P10	26	9-Oct	4-Dec	57O	569.3	**574.0**
P10	26	9-Oct	4-Dec	57P	578.7	
P7	3	13-Aug	8-Oct	11O	612.1	**598.9**
P7	3	13-Aug	8-Oct	11P	585.7	
P6	10	13-Aug	8-Oct	18G	852.0	**885.8**
P6	10	13-Aug	8-Oct	18H	919.5	
P6	11	17-Aug	12-Oct	22G	852.5	**838.0**
P6	11	17-Aug	12-Oct	22H	823.4	
P6	12	18-Aug	13-Oct	25G	836.3	**860.1**
P6	12	18-Aug	13-Oct	25H	883.8	
P6	13	2-Sep	28-Oct	26G	1245.4	**1265.9**
P6	13	2-Sep	28-Oct	26H	1286.3	
P6	14	3-Sep	29-Oct	28G	978.4	**965.8**
P6	14	3-Sep	29-Oct	28H	953.2	
P1	1	20-Aug	15-Oct	1G	810.5	**830.4**
P1	1	20-Aug	15-Oct	1H	850.3	
P1	2	26-Aug	21-Oct	2G	710.1	**701.4**
P1	2	26-Aug	21-Oct	2H	692.6	
P1	3	28-Aug	23-Oct	3G	1012.9	**1034.2**
P1	3	28-Aug	23-Oct	3H	1055.4	

P1	4	31-Aug	26-Oct	4G	1041.3	**1036.0**
P1	4	31-Aug	26-Oct	4H	1030.6	
P1	5	2-Sep	28-Oct	5G	830.7	**808.8**
P1	5	2-Sep	28-Oct	5H	786.8	
P1	6	4-Sep	30-Oct	6G	647.8	**614.6**
P1	6	4-Sep	30-Oct	6H	581.3	
P1	7	16-Sep	12-Nov	7G	1301.8	**1300.8**
P1	7	16-Sep	12-Nov	7H	1299.7	
P1	8	24-Sep	19-Nov	8G	652.2	**667.8**
P1	8	24-Sep	19-Nov	8H	683.4	
P1	9	25-Sep	19-Nov	9G	1241.5	**1202.4**
P1	9	25-Sep	19-Nov	9H	1163.2	
P1	10	2-Oct	27-Nov	10G	578.9	**573.5**
P1	10	2-Oct	27-Nov	10H	568.0	
P1	11	8-Oct	3-Dec	11G	461.9	**484.7**
P1	11	8-Oct	3-Dec	11H	507.4	
P1	12	15-Oct	10-Dec	12G	441.0	**437.6**
P1	12	15-Oct	10-Dec	12H	434.1	
P4	2	28-Sep	23-Nov	3N	422.9	**407.7**
P4	2	28-Sep	23-Nov	3O	392.5	
P4	3	5-Oct	30-Nov	6L	488.6	**465.5**
P4	3	5-Oct	30-Nov	6M	442.4	
P4	4	7-Oct	2-Dec	8L	492.4	**490.8**
P4	4	7-Oct	2-Dec	8M	489.2	
P4	5	12-Oct	7-Dec	9L	471.1	**491.2**
P4	5	12-Oct	7-Dec	9M	511.2	
P4	6	14-Oct	9-Dec	12L	472.3	**480.4**
P4	6	14-Oct	9-Dec	12M	488.4	
P4	7	15-Oct	10-Dec	14L	612.5	**612.9**
P4	7	15-Oct	10-Dec	14M	613.2	
P2	3	10-Oct	5-Dec	5G	748.1	**714.1**
P2	3	10-Oct	5-Dec	7G	665.2	
P5	26	21-Oct	15-Dec	47G	680.0	**655.8**
P5	26	21-Oct	15-Dec	47H	631.6	
P4	8	21-Oct	16-Dec	17N	512.1	**526.8**
P4	8	21-Oct	16-Dec	18K	541.5	
P3	5	16-Oct	11-Dec	12O	527.1	**527.1**
P3	9	12-Nov	7-Jan	18O	426.4	**426.4**
P3	9	12-Nov	7-Jan			
P3	10	13-Nov	8-Jan	20O	380.6	**380.6**

P8	6	10-Nov	12-Jan	6O	710.9	**684**
P11	1	13-Nov	7-Sep	1H	5790.0	**5790**
P11	1	10-Nov	7-Sep	1I	5402.0	**5402**
P12	1	27-Oct	5-Jan	1	1094.0	**1094.0**
P12	1	27-Oct	6-Jan	2	1123.0	**1123.0**
P12	1	27-Oct	6-Jan			
L1	Lab	22-Feb-18	19-Apr-18		7349.0	**7349**
L1	Lab	22-Feb-18	19-Apr-18		7349.0	
L2	Lab	22-Feb-18	19-Apr-18		4471.0	
L2	Lab	22-Feb-18	19-Apr-18		4471.0	**4471**
L3	Lab	30-Apr-18	25-Jun-18		2518.1	
L3	Lab	30-Apr-18	25-Jun-18		2518.1	**2518.1**
L4	Lab	30-Apr-18	25-Jun-18		2518.1	
L4	Lab	30-Apr-18	25-Jun-18		2213.1	**2213.1**
L4	Lab	30-Apr-18	25-Jun-18		2213.1	
L6	Lab	30-Apr-18	25-Jun-18		313.9	**313.9**
L5	Lab	30-Apr-18	25-Jun-18		812.2	**812.2**
P13	33	3-May-18	28-Jun-18	66I	910.3	**910.3**
P13	36	30-May-18	25-Jul-18	72I	637.1	**637.1**

APPENDIX E – Temperature Treatment Data

	Temperature Treatment Data									
	Mix 2 (5% Fly Ash)					Mix 4 (20% FA, 5% SF)				
Specimen Temperature (°C)	60	38	23	-2	-18	60	38	23	-2	-18
Measurements @ 0, 90, 180 & 270 degrees	6.8	8	16.9	37.3	155.4	30.5	40.9	44.9	86.9	307
	6.9	8.2	16.8	37.2	144	29.5	39.5	46.4	85.1	328
	6.4	8	16.8	35.5	122.4	31.5	40.1	44.3	82.1	293
	6.8	8.1	16.6	36.4	128	30.5	40.4	45.5	91.6	318
	6.8	8	17.6	36	143	31.3	40.5	45.1	87.6	315
	6.7	8.2	16.2	37.4	132	31.5	41.7	47.4	82.1	279
	6.8	8.4	17.2	36.2	120	30	44.1	46.2	85.4	280
	7.1	7.9	16.1	34.1	128	34	42.9	48.1	84.4	315
Avg. Surface Resistivity (kΩ-cm)	6.8	8.1	16.8	36.3	134.1	31.1	41.3	46.0	85.7	304.4
Temperature (Kelvin)	333.2	311.2	296.2	271.2	255.2	333.2	311.2	296.2	271.2	255.2
Temperature (Normalized to 23C) (kΩ-cm)	2.3	5.1	16.8	89.6	647.9	10.5	25.8	46.1	211.6	1470.6
Error	-66%	-38%	0%	147%	383%	-66%	-38%	0%	147%	383%

Curriculum Vitae

Candidates Full Name:

Matthew Clifford MacArthur

Universities Attended:

University of New Brunswick, 2005-2010, BScE

Publications: None

Conference Presentations: None